Thermodynamics and quark condensates of three-flavor QCD at low temperature

Jens O. Andersen,[1,*] Qing Yu,[2,1,†] and Hua Zhou[2,1,‡]

[1]*Department of Physics, Faculty of Natural Sciences, NTNU, Norwegian University of Science and Technology, Høgskoleringen 5, N-7491 Trondheim, Norway*

[2]*Department of Physics, Chongqing University, Chongqing 401331, People's Republic of China*

(Received 18 July 2022; accepted 2 December 2022; published 6 January 2023)

We use three-flavor chiral perturbation theory (χPT) to calculate the pressure, light, and s-quark condensates of QCD in the confined phase at finite temperature to $\mathcal{O}(p^6)$ in the low-energy expansion. We also include electromagnetic effects to order e^2, where the electromagnetic coupling e counts as order p. Our results for the pressure and the condensates suggest that χPT converges very well for temperatures up to approximately 150 MeV. We combine χPT and the hadron resonance gas (HRG) model by adding heavier baryons and mesons. Our results are compared with lattice simulations and the agreement is very good for temperatures below 170 MeV, in contrast to the results from χPT which agree with the lattice only up to $T \approx 120$ MeV. Our value for the chiral crossover temperature is 160.1 MeV, which compares favorably to the lattice result of 157.3 MeV.

DOI: 10.1103/PhysRevD.107.014010

I. INTRODUCTION

In massless QCD with three flavors, the QCD Lagrangian has a global $SU(3)_L \times SU(3)_R \times U(1)_B$ symmetry in addition to a local $SU(N_c)$ gauge symmetry. In the vacuum, this symmetry is broken down to $SU(3)_V \times U(1)_B$ via the formation of a quark condensate, which gives rise to eight massless Goldstone bosons, the charged and neutral pions, the charged and neutral kaons, and the eta. In nature, this symmetry is explicitly broken by finite quark masses down to $SU(2)_V \times U(1)_Y \times U(1)_B$ giving rise to pseudo-Goldstone bosons whose masses are small compared to the typical hadronic scale. The low-energy effective theory that describes the pseudo-Goldstone bosons is chiral perturbation theory (χPT), which is based only on the global symmetries of QCD and the low-energy degrees of freedom [1–3]. It therefore provides a model-independent framework for describing the low-energy dynamics of QCD.

The original formulation of χPT was in the strong sector. Gasser and Leytwyler developed a consistent power counting scheme such that the effective Lagrangian can be written as an infinite series of terms in a low-energy expansion. The leading-order Lagrangian is simply the nonlinear sigma model. The next-to-leading order Lagrangian for two flavors was derived in Ref. [2] and for three flavors in Ref. [3]. At next-to-next-to leading order, the effective Lagrangian was derived in Refs. [4–6]. A review of the phenomenology of chiral perturbation theory was given in Ref. [7].

In the strong sector, the charged and neutral pions have the same tree-level masses. A mass difference between the u and the d quarks, produces isospin breaking effects in hadron masses. For pions, this effect is second order in $m_u - m_d$. For charged and neutral kaons it turns out that their mass difference is linear in the quark mass difference $m_u - m_d$. However, there is another important source of the mass differences between the neutral and charged mesons, namely the effects of virtual photons. The leading electromagnetic effects of order e^2 were first included in Ref. [8], while the systematic inclusion of the effects of virtual photons in χPT at next-to-leading order, i.e., $\mathcal{O}(e^2p^2)$ and $\mathcal{O}(e^4)$ was carried out in Refs. [9–12]. The power counting rule in χPT developed in [9] is such that e counts as order p.

Given the success of chiral perturbation theory at $T = 0$, one may hope that it also provides a good description of the QCD thermodynamics at low temperature. In the chiral limit, the pions are massless and their typical momenta are of order T. If T is sufficiently small, the low-energy expansion ought to converge. Again, in the massless limit, the pion decay constant f is the only scale that appears in the leading-order Lagrangian. Up to corrections given by the low-energy constants that appear at higher orders in the low-energy expansion, T/f is the expansion parameter of χPT. In a series of papers, the low-temperature

*andersen@tf.phys.ntnu.no
†yuq@cqu.edu.cn
‡zhouhua@cqu.edu.cn

expansions of the pressure $\mathcal{P}$ and quark condensate $\langle\bar{q}q\rangle$ in two-flavor χPT were calculated and show the expected form [13–15]

$$\mathcal{P} = \frac{\pi^2 T^4}{30}\left[1 + \frac{1}{36}\frac{T^4}{f^4}\log\frac{\Lambda_p}{T} + \mathcal{O}\left(\frac{T^6}{f^6}\right)\right], \tag{1}$$

$$\langle\bar{q}q\rangle = \langle\bar{q}q\rangle_0\left[1 - \frac{1}{8}\frac{T^2}{f^2} - \frac{1}{384}\frac{T^4}{f^4} - \frac{1}{288}\frac{T^6}{f^6}\log\frac{\Lambda_q}{T} + \mathcal{O}\left(\frac{T^8}{f^8}\right)\right], \tag{2}$$

where $\langle\bar{q}q\rangle_0$ is condensate in the vacuum, $\Lambda_p = 275 \pm 65$ MeV and $\Lambda_q = 470 \pm 110$ MeV [15]. Λ_p and Λ_q depend on the low-energy constants $\overline{l}_i$, which up to a factor are the running couplings $l_i^r(\Lambda)$ evaluated at the scale $\Lambda = m$, m being the (bare) pion mass. The expansions show good convergence properties for temperatures up to approximately 140 MeV [15].

However, at high enough temperature, χPT ceases to be valid since other degrees of freedom are excited and one must use other methods. Lattice Monte Carlo techniques is a first-principles method that can be used to study finite-temperature QCD: At zero (and small) baryon chemical potential, one can carry out lattice simulations to calculate thermodynamic quantities such as the pressure and interaction measure as well as the approximate order parameters that characterize confinement and chiral symmetry breaking, namely the Polyakov loop and the quark condensates. For physical quark masses and two quark flavors, the transition is a smooth crossover at a transition temperature of around 155 MeV [16–19].

The hadron resonance gas (HRG) model treats finite-temperature QCD as a gas of noninteracting hadrons and their resonances. As T gets higher, it is necessary to include more and more particles, and typically one has included the approximately 200 hadrons below 2.5 GeV. It can be easily generalized to finite chemical potentials as well as be "distorted" by using not the physical masses but masses that take into account lattice discretization effects. It has also been combined with results from two-flavor χPT by adding the contributions from heavier hadrons [18]. Comparing predictions for e.g. the pressure and the quark condensate of lattice QCD and the HRG model, one finds, perhaps surprisingly, very good agreement given the fact that the latter does not include interactions (unless combined with e.g. χPT) [18,20–23].

Finite temperature calculations within χPT including electromagnetic effects are scarce. In Ref. [24], the authors calculate the quark condensates at NLO in two-flavor and three-flavor χPT. In Ref. [25], they calculate the pole masses and the damping rate for the charged pion in two-flavor χPT at LO in the classes of covariant and Coulomb gauges. While the pole mass is gauge-fixing independent in the two classes of gauges and coincide, the damping rate depends on the gauge. In particular, the damping rate in covariant gauge is negative indicating an instability. This is reminiscent of the old problem of the gauge dependence of the gluon damping rate in hot QCD. The problem was solved by Braaten and Pisarski who realized that a one-loop calculation is incomplete and that one must use effective propagators and vertices to obtain a complete leading-order result [26,27]. This is summarized in a nonlocal effective Lagrangian that upon expansion generates the correction terms [28,29]. This Lagrangian has been generalized to all temperatures and densities in Ref. [30] and can possibly be used to resolve the gauge dependence of the damping rate in χPT.

In the present paper, we consider three-flavor χPT at finite temperature including electromagnetic effects to leading order in e^2. We calculate the pressure and the quark condensates to $\mathcal{O}(p^6)$. In order to extend the validity of our calculations to higher temperatures, we combine the results from χPT and the hadron resonance gas model. The latter has enjoyed considerable success in describing the thermodynamics of low-temperature QCD as obtained from the lattice. The paper is organized as follows. In Sec. II, we briefly discuss the chiral Lagrangian. In Sec. III, we calculate the pressure to $\mathcal{O}(p^6)$ in the low-energy expansion. In Sec. IV, we discuss the extension of the chiral Lagrangian to include the effects of electromagnetic interactions. In Sec. V, the pressure is again calculated to $\mathcal{O}(p^6)$ in the low-energy expansion. In Sec. VI, we calculate the quark condensates while in Sec. VII we briefly discuss the hadron resonance gas model. In Sec. VIII, we present and discuss our numerical results. We have included four appendices providing the reader with definitions and useful calculational details. In particular, we calculate the quark condensate at $T = 0$ including electromagnetic effects, which is required in the calculation of the finite-temperature dependent quark condensates.

II. CHIRAL LAGRANGIAN

In massless three-flavor QCD, the Lagrangian has a global $SU(3)_L \times SU(3)_R$ symmetry in addition to the global $U(1)_B$ baryon symmetry and the local $SU(N_c)$ gauge symmetry. In the vacuum, this symmetry is broken to $SU(3)_V$ by the formation of a quark condensates. For two massless and one massive quark, the symmetry is $SU(2)_L \times SU(2)_R$, which is broken to $SU(2)_V$ in the vacuum. For two degenerate light quarks and one massive quark, this symmetry is explicit broken to $SU(2)_V$. If the two quarks are nondegenerate, we have three $U(1)$ symmetries, one for each quark flavor.

Chiral perturbation theory is a low-energy effective theory of QCD which is based on the global symmetries and relevant degrees of freedom [1–3]. For three-flavor QCD, the degrees of freedom are the eight mesons: three

pions, four kaons, and the η. In the chiral Lagrangian each factor of a quark mass counts two powers of momentum and each factor of a derivative counts one power of momentum. The leading-order Lagrangian is given by [3]

$$\mathcal{L}_2 = \frac{1}{4}f^2\langle\partial_\mu\Sigma\partial^\mu\Sigma^\dagger\rangle + \frac{1}{4}f^2\langle\chi^\dagger\Sigma + \Sigma^\dagger\chi\rangle, \tag{3}$$

where $\langle A\rangle$ denotes the trace of a matrix A in flavor space, f is the bare pion decay constant, and χ is given in terms of the quark mass matrix

$$\chi = 2B_0\mathrm{diag}(m_u, m_d, m_s). \tag{4}$$

Finally,

$$\Sigma = \exp\left[i\frac{\lambda_a\phi_a}{f}\right], \tag{5}$$

with ϕ_a being the meson fields parametrizing the Goldstone manifold and where λ_a are the Gell-Mann matrices that satisfy $\langle\lambda_a\lambda_b\rangle = 2\delta_{ab}$.

Expanding the Lagrangian $\mathcal{L}_2$ to second order in the fields ϕ_a, we find

$$\begin{aligned}\mathcal{L}_2^{\mathrm{quadratic}} &= \partial_\mu\pi^+\partial^\mu\pi^- - m_{\pi,0}^2\pi^+\pi^- + \frac{1}{2}\partial_\mu\pi^0\partial^\mu\pi^0 \\ &\quad - \frac{1}{2}m_{\pi,0}^2(\pi^0)^2 + \partial_\mu K^+\partial^\mu K^- \\ &\quad - m_{K^\pm,0}^2K^+K^- + \partial_\mu K^0\partial^\mu\overline{K}^0 - m_{K^0,0}^2K^0\bar{K}^0 \\ &\quad + \frac{1}{2}\partial_\mu\eta\partial^\mu\eta - \frac{1}{2}m_{\eta,0}^2\eta^2,\end{aligned} \tag{6}$$

where the meson fields are expressed in terms of ϕ_a as

$$\pi^\pm = \frac{1}{\sqrt{2}}(\phi_1 \mp i\phi_2), \tag{7}$$

$$\pi^0 = \phi_3, \tag{8}$$

$$K^\pm = \frac{1}{\sqrt{2}}(\phi_4 \mp i\phi_5), \tag{9}$$

$$K^0/\bar{K}^0 = \frac{1}{\sqrt{2}}(\phi_6 \mp i\phi_7), \tag{10}$$

$$\eta = \phi_8. \tag{11}$$

The tree-level masses are

$$m_{\pi,0}^2 = B_0(m_u + m_d), \tag{12}$$

$$m_{K^\pm,0}^2 = B_0(m_u + m_s), \tag{13}$$

$$m_{K^0,0}^2 = B_0(m_d + m_s), \tag{14}$$

$$m_{\eta,0}^2 = \frac{B_0(m_u + m_d + 4m_s)}{3}. \tag{15}$$

Since we are working in the isospin limit, there is no mixing between π^0 and η. As long as $e = 0$, the charged and neutral kaons have the same bare mass which is denoted by $m_{K,0}$.

The quartic terms of the Lagrangian $\mathcal{L}_2$ contains a large number of terms. They can conveniently be written as

$$\begin{aligned}\mathcal{L}_2^{\mathrm{quartic}} =& \frac{m_{\pi,0}^2}{24f^2}(\pi^0)^4 + \frac{m_{\pi,0}^2}{12f^2}(\pi^0)^2\eta^2 + \frac{m_{\pi,0}^2}{6f^2}\pi^+\pi^-\eta^2 + \frac{1}{216f^2}(16m_{K,0}^2 - 7m_{\pi,0}^2)\eta^4 - \frac{1}{6f^2}[2(\pi^0)^2\partial_\mu\pi^+\partial^\mu\pi^- + 2\pi^+\pi^-\partial_\mu\pi^0\partial^\mu\pi^0 \\ &- m_{\pi,0}^2\pi^+\pi^-(\pi^0)^2] - \frac{1}{6f^2}\pi^+\pi^-[2\partial_\mu\pi^+\partial^\mu\pi^- - m_{\pi,0}^2\pi^+\pi^-] - \frac{1}{6f^2}K^+K^-[2\partial_\mu K^+\partial^\mu K^- - m_{K,0}^2K^+K^-] \\ &- \frac{1}{6f^2}\pi^+\pi^-[\partial_\mu K^+\partial^\mu K^- - m_{K,0}^2K^+K^-] - \frac{1}{6f^2}K^+K^-[\partial_\mu\pi^+\partial^\mu\pi^- - m_{\pi,0}^2\pi^+\pi^-] - \frac{1}{6f^2}[2K^0\bar{K}^0\partial_\mu K^0\partial^\mu\bar{K}^0 - m_{K,0}^2(K^0\bar{K}^0)^2] \\ &- \frac{1}{12f^2}[K_0\bar{K}_0\partial_\mu\pi_0\partial^\mu\pi_0 + (\pi^0)^2\partial_\mu K_0\partial^\mu\bar{K}_0 - (m_{\pi,0}^2 + m_{K,0}^2)(\pi^0)^2K_0\bar{K}^0] - \frac{1}{12f^2}[K^+K^-\partial_\mu\pi_0\partial^\mu\pi_0 + (\pi^0)^2\partial_\mu K^+\partial^\mu K^- \\ &- (m_{\pi,0}^2 + m_{K,0}^2)(\pi^0)^2K^+K^-] - \frac{1}{6f^2}[K^0\bar{K}^0\partial_\mu\pi^+\partial^\mu\pi^- + \pi^+\pi^-\partial_\mu K^0\partial^\mu\bar{K}^0 - (m_{\pi,0}^2 + m_{K,0}^2)\pi^+\pi^-K^0\bar{K}^0] \\ &- \frac{1}{6f^2}[K^+K^-\partial_\mu K^0\partial^\mu\bar{K}^0 + K^0\bar{K}^0\partial_\mu K^+\partial^\mu K^- - 2m_{K,0}^2K^+K^-K^0\bar{K}^0] - \frac{1}{12f^2}[3K^+K^-\partial_\mu\eta\partial^\mu\eta + 3\eta^2\partial_\mu K^+\partial^\mu K^- \\ &+ (m_{\pi,0}^2 - 3m_{K,0}^2)K^+K^-\eta^2] - \frac{1}{12f^2}[3K^0\bar{K}^0\partial_\mu\eta\partial^\mu\eta + 3\eta^2\partial_\mu K^0\partial^\mu\bar{K}^0 + (m_{\pi,0}^2 - 3m_{K,0}^2)K^0\bar{K}^0\eta^2],\end{aligned} \tag{16}$$

where we have omitted terms that do not contribute to the pressure or quark condensates at two loops in the isospin limit.

At next-to-leading order in the low-energy expansion, there are 12 terms in the chiral Lagrangian [3]. The terms that are relevant for the present calculations are

$$\begin{aligned}\mathcal{L}_4 &= L_4\langle\partial_\mu\Sigma^\dagger\partial^\mu\Sigma\rangle\langle\chi^\dagger\Sigma+\chi\Sigma^\dagger\rangle \\ &+ L_5\langle(\partial_\mu\Sigma^\dagger\partial^\mu\Sigma)(\chi^\dagger\Sigma+\chi\Sigma^\dagger)\rangle \\ &+ L_6\langle\chi^\dagger\Sigma+\chi\Sigma^\dagger\rangle^2 + L_7\langle\chi\Sigma^\dagger-\chi^\dagger\Sigma\rangle^2 \\ &+ L_8\langle\chi^\dagger\Sigma\chi^\dagger\Sigma+\chi\Sigma^\dagger\chi\Sigma^\dagger\rangle + H_2\langle\chi\chi^\dagger\rangle, \end{aligned} \tag{17}$$

where L_i are the so-called low-energy constants ($i=0,1,2\ldots10$), H_i are the coefficients of the contact terms in chiral Lagrangian, and referred to as high-energy constants ($i=1,2$). The relations between the bare couplings L_i and H_i and their renormalized counterparts L_i^r and H_i^r are

$$L_i = L_i^r - \frac{\Gamma_i\Lambda^{-2\epsilon}}{2(4\pi)^2}\left[\frac{1}{\epsilon}+1\right], \tag{18}$$

$$H_i = H_i^r - \frac{\Delta_i\Lambda^{-2\epsilon}}{2(4\pi)^2}\left[\frac{1}{\epsilon}+1\right]. \tag{19}$$

The constants Γ_i and Δ_i assume the following values [3]

$$\Gamma_4=\frac{1}{8}, \qquad \Gamma_5=\frac{3}{8}, \qquad \Gamma_6=\frac{11}{144}, \tag{20}$$

$$\Gamma_7=0, \qquad \Gamma_8=\frac{5}{48}, \qquad \Delta_2=\frac{5}{24}. \tag{21}$$

Since the bare parameters are independent of the scale Λ, differentiation of Eqs. (18) and (19) immediately gives rise to equations governing the running of the renormalized couplings. The renormalization group equations read

$$\Lambda\frac{dL_i^r}{d\Lambda} = -\frac{\Gamma_i}{(4\pi)^2}, \qquad \Lambda\frac{dH_i^r}{d\Lambda} = -\frac{\Delta_i}{(4\pi)^2}. \tag{22}$$

We note that $\Gamma_7=0$, which implies that L_7^r does not run and we write $L_7=L_7^r$.

The quadratic part of the Lagrangian Eq. (17) is given by

$$\begin{aligned}\mathcal{L}_4^{\text{quadratic}} &= \frac{4L_4}{f^2}(m_{\pi,0}^2+2m_{K,0}^2)[2\partial_\mu\pi^+\partial^\mu\pi^- + \partial_\mu\pi^0\partial^\mu\pi^0 + 2\partial_\mu K^+\partial^\mu K^- + 2\partial_\mu K^0\partial^\mu\bar{K}^0 + \partial_\mu\eta\partial^\mu\eta] \\ &+ \frac{4L_5}{f^2}[m_{\pi,0}^2(2\partial_\mu\pi^+\partial^\mu\pi^- + \partial_\mu\pi^0\partial^\mu\pi^0) + 2m_{K,0}^2(\partial_\mu K^+\partial^\mu K^- + \partial_\mu K^0\partial^\mu\bar{K}^0) + m_{\eta,0}^2\partial_\mu\eta\partial^\mu\eta] \\ &- \frac{8L_6}{f^2}(m_{\pi,0}^2+2m_{K,0}^2)[m_{\pi,0}^2(2\pi^+\pi^- + (\pi^0)^2) + 2m_{K,0}^2(K^+K^- + K^0\bar{K}^0) + m_{\eta,0}^2\eta^2] \\ &- \frac{64L_7}{3f^2}(m_{\pi,0}^2-m_{K,0}^2)^2\eta^2 - \frac{16L_8}{f^2}\left[m_{\pi,0}^4\pi^+\pi^- + \frac{1}{2}m_{\pi,0}^4(\pi^0)^2 + m_{K,0}^4(K^+K^- + K^0\bar{K}^0)\right. \\ &\left. + \frac{1}{3}\left(4m_{K,0}^4 - 4m_{\pi,0}^2m_{K,0}^2 + \frac{3}{2}m_{\pi,0}^4\right)\eta^2\right]. \end{aligned} \tag{23}$$

Finally, there are static terms from $\mathcal{L}_6$ that contribute at $\mathcal{O}(p^6)$ to the pressure, but they are temperature independent and only serve to renormalize the vacuum energy.

III. PRESSURE

The free energy density is given by

$$\mathcal{F} = -\frac{T}{V_{\text{sys}}}\log\mathcal{Z}, \tag{24}$$

where V_{sys} is the volume of the system and $\mathcal{Z}$ is the partition function which can be expressed as a path integral in the imaginary-time formalism

$$\mathcal{Z} = \int\mathcal{D}\phi e^{-\int_0^\beta d\tau\int d^3x\mathcal{L}_E}, \tag{25}$$

where $\mathcal{L}_E$ is the Euclidean Lagrangian, $\beta\equiv1/T$, and ϕ is short-hand notation for all the fields integrated over. The pressure is then given by $\mathcal{P}=-\mathcal{F}$. The loop diagrams that contribute to the pressure are ultraviolet divergent and must be regularized. We use dimensional regularization where power divergences are set to zero and logarithmic divergences show up as poles in ϵ, where $d=3-2\epsilon$. There are both temperature-independent and temperature-dependent divergences. The counterterms diagrams that are used to cancel the $T=0$ divergences are also sufficient to cancel the temperature-dependent ones. In the present paper, we

are interested in finite-temperature effects and so we simply throw away the $T = 0$ divergences.

The $\mathcal{O}(p^2)$ contribution is given by the static part of the Lagrangian $\mathcal{L}_2$. Since this term is temperature independent, we ignore it henceforth. In the following, we denote the finite-temperature contribution at $\mathcal{O}(p^{2n})$ by $\mathcal{P}_{n-1}$ with $n = 1, 2, 3\ldots$. The result through $\mathcal{O}(p^{2n})$ is denoted by $\mathcal{P}_{0+1+\cdots n-1}$.

A. $\mathcal{O}(p^4)$

The one-loop pressure is given by

$$\mathcal{P}_1 = \frac{3}{2} I_0'(m_{\pi,0}^2) + 2I_0'(m_{K,0}^2) + \frac{1}{2} I_0'(m_{\eta,0}^2), \quad (26)$$

where $I_0'(m)$ is given by Eq. (A6). Since we are only interested in the temperature dependence, we keep the terms $J_0(\beta m)$ to obtain

$$\mathcal{P}_{0+1} = \frac{T^4}{(4\pi)^2}\left[\frac{3}{2} J_0(\beta m_{\pi,0}) + 2J_0(\beta m_{K,0}) + \frac{1}{2} J_0(\beta m_{\eta,0})\right], \quad (27)$$

where the thermal integrals $J_n(\beta m)$ are defined in Eq. (A8) and where $J_0(\beta m)$ is to be evaluated at $\epsilon = 0$.

B. $\mathcal{O}(p^6)$

At $\mathcal{O}(p^6)$, there are three contributions to the pressure: the tree-level graphs, the one-loop graphs with a mass or derivative insertion, and the two-loop graphs. The tree graphs are temperature independent and discarded. The one-loop diagrams can be split into a temperature-independent term and a temperature-dependent term, where both of them are divergent. The two-loop graphs can be split in a similar manner. The temperature-dependent divergent parts from the one-loop graphs cancel against the temperature-dependent divergent parts from the two-loop graphs, showing that renormalization at $T = 0$ is sufficient to obtain a finite expression for the pressure.

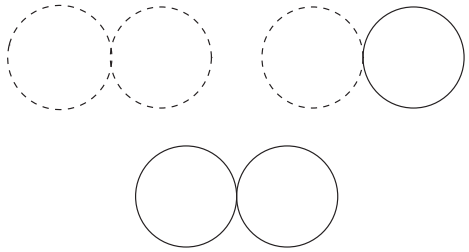

FIG. 1. Two-loop Feynman graphs contributing to the pressure at $\mathcal{O}(p^6)$. Dashed line represents a neutral meson and solid line represents a charged meson.

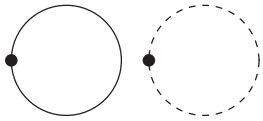

FIG. 2. One-loop Feynman graphs with a mass or derivate counterterm insertion (indicated by a black blob) contributing to the pressure at $\mathcal{O}(p^6)$.

The two-loop graphs are shown in the Fig. 1. Their expression is

$$\mathcal{P}_2^a = -\frac{m_{\pi,0}^2}{f^2}\left[\frac{3}{8} I_1^2(m_{\pi,0}^2) - \frac{1}{4} I_1(m_{\pi,0}^2) I_1(m_{\eta,0}^2) + \frac{7}{72} I_1^2(m_{\eta,0}^2)\right] - \frac{m_{K,0}^2}{f^2}\left[\frac{2}{3} I_1(m_{K,0}^2) I_1(m_{\eta,0}^2) - \frac{2}{9} I_1^2(m_{\eta,0}^2)\right], \quad (28)$$

where the integral $I_1(m^2)$ is defined in Eq. (A7). The one-loop counterterm graphs are shown in Fig. 2. Their expression is

$$\begin{aligned}\mathcal{P}_2^b = {} & \frac{4L_4 - 8L_6}{f^2}(m_{\pi,0}^2 + 2m_{K,0}^2)[3m_{\pi,0}^2 I_1(m_{\pi,0}^2) + 4m_{K,0}^2 I_1(m_{K,0}^2) + m_{\eta,0}^2 I_1(m_{\eta,0}^2)] \\ & + \frac{4L_5}{f^2}[3m_{\pi,0}^4 I_1(m_{\pi,0}^2) + 4m_{K,0}^4 I_1(m_{K,0}^2) + m_{\eta,0}^4 I_1(m_{\eta,0}^2)] - \frac{64L_7}{3f^2}(m_{\pi,0}^2 - m_{K,0}^2)^2 I_1(m_{\eta,0}^2) \\ & - \frac{8L_8}{f^2}\left[3m_{\pi,0}^4 I_1(m_{\pi,0}^2) + 4m_{K,0}^4 I_1(m_{K,0}^2) + \frac{8m_{K,0}^4 - 8m_{K,0}^2 m_{\pi,0}^2 + 3m_{\pi,0}^4}{3} I_1(m_{\eta,0}^2)\right]. \end{aligned} \quad (29)$$

Adding Eqs. (28) and (29), and renormalizing the couplings using Eq. (18), we obtain

$$\mathcal{P}_2 = -\frac{m_{\pi,0}^2 T^4}{(4\pi)^4 f^2}\left[\frac{3}{8}J_1^2(\beta m_{\pi,0}) - \frac{1}{4}J_1(\beta m_{\pi,0})J_1(\beta m_{\eta,0}) + \frac{7}{72}J_1^2(\beta m_{\eta,0})\right] - \frac{m_{K,0}^2 T^4}{(4\pi)^4 f^2}\left[\frac{2}{3}J_1(\beta m_{K,0})J_1(\beta m_{\eta,0}) - \frac{2}{9}J_1^2(\beta m_{\eta,0})\right]$$
$$+ \frac{(4L_4^r - 8L_6^r)T^2}{(4\pi)^2 f^2}(m_{\pi,0}^2 + 2m_{K,0}^2)[3m_{\pi,0}^2 J_1(\beta m_{\pi,0}) + 4m_{K,0}^2 J_1(\beta m_{K,0}) + m_{\eta,0}^2 J_1(\beta m_{\eta,0})]$$
$$+ \frac{4L_5^r T^2}{(4\pi)^2 f^2}[3m_{\pi,0}^4 J_1(\beta m_{\pi,0}) + 4m_{K,0}^4 J_1(\beta m_{K,0}) + m_{\eta,0}^4 J_1(\beta m_{\eta,0})] - \frac{64L_7^r T^2}{3(4\pi)^2 f^2}(m_{\pi,0}^2 - m_{K,0}^2)^2 J_1(\beta m_{\eta,0})$$
$$- \frac{8L_8^r T^2}{(4\pi)^2 f^2}\left[3m_{\pi,0}^4 J_1(\beta m_{\pi,0}) + 4m_{K,0}^4 J_1(\beta m_{K,0}) + \frac{1}{3}(8m_{K,0}^4 - 8m_{\pi,0}^2 m_{K,0}^2 + 3m_{\pi,0}^4)J_1(\beta m_{\eta,0})\right]$$
$$+ \frac{T^2 J_1(\beta m_{\pi,0})}{(4\pi)^4 f^2}\left(\frac{3}{4}m_{\pi,0}^4 \log\frac{\Lambda^2}{m_{\pi,0}^2} - \frac{1}{4}m_{\pi,0}^2 m_{\eta,0}^2 \log\frac{\Lambda^2}{m_{\eta,0}^2}\right) + \frac{T^2 J_1(\beta m_{K,0})}{(4\pi)^4 f^2}\left(\frac{2}{3}m_{K,0}^2 m_{\eta,0}^2 \log\frac{\Lambda^2}{m_{\eta,0}^2}\right)$$
$$+ \frac{T^2 J_1(\beta m_{\eta,0})}{(4\pi)^4 f^2}\left(-\frac{1}{4}m_{\pi,0}^4 \log\frac{\Lambda^2}{m_{\pi,0}^2} + \frac{2}{3}m_{K,0}^4 \log\frac{\Lambda^2}{m_{K,0}^2} - \frac{1}{3}m_{\eta,0}^4 \log\frac{\Lambda^2}{m_{\eta,0}^2} + \frac{1}{12}m_{\pi,0}^2 m_{\eta,0}^2 \log\frac{\Lambda^2}{m_{\eta,0}^2}\right), \tag{30}$$

where $J_1(\beta m)$ is to be evaluated at $\epsilon = 0$.

The terms proportional to the renormalized couplings L_i^r and the logarithms can be absorbed in the one-loop result by replacing the bare meson masses with the physical meson masses at one loop, listed in Appendix D. This can be seen by writing the meson masses schematically as $m^2 + \delta m^2$ and expanding the one-loop contribution as

$$I_0'(m^2 + \delta m^2) = I_0'(m^2) - \delta m^2 I_1(m^2), \tag{31}$$

where we have used Eq. (A5). Similarly, using Eq. (A9) for $\epsilon = 0$, we find

$$J_0(\beta\sqrt{m^2 + \delta m^2}) = J_0(\beta m) - \delta m^2 \beta^2 J_1(\beta m). \tag{32}$$

The sum of Eqs. (27) and (30) gives in the limit $\epsilon \to 0$, the finite-temperature pressure through $\mathcal{O}(p^6)$

$$\mathcal{P}_{0+1+2} = \frac{T^4}{(4\pi)^2}\left[\frac{3}{2}J_0(\beta M_\pi) + 2J_0(\beta M_K) + \frac{1}{2}J_0(\beta M_\eta)\right]$$
$$- \frac{m_{\pi,0}^2 T^4}{(4\pi)^4 f^2}\left[\frac{3}{8}J_1^2(\beta m_{\pi,0}) - \frac{1}{4}J_1(\beta m_{\pi,0})J_1(\beta m_{\eta,0}) + \frac{7}{72}J_1^2(\beta m_{\eta,0})\right] - \frac{m_{K,0}^2 T^4}{(4\pi)^4 f^2}\left[\frac{2}{3}J_1(\beta m_{K,0})J_1(\beta m_{\eta,0}) - \frac{2}{9}J_1^2(\beta m_{\eta,0})\right]. \tag{33}$$

We note that the result simplifies significantly in the chiral limit since the terms proportional to $m_{\pi,0}^2$ vanish. In the two-flavor case, the correction to the Stefan-Boltzmann result is of $\mathcal{O}(p^8)$, cf. Eq. (1).

IV. INCLUDING ELECTROMAGNETIC INTERACTIONS

Electromagnetic interactions in the framework of chiral perturbation theory were first included by Urech in Ref. [9] in the three-flavor case. The $SU(2)_V$ symmetry of the chiral Lagrangian is then becoming a local $U(1)$ gauge symmetry. Moreover, he showed that one can find a consistent power counting scheme also in this case, if the electromagnetic coupling e counts as $\mathcal{O}(p)$ and the electromagnetic field A_μ counts as $\mathcal{O}(1)$. The leading-order Lagrangian is now given by [8]

$$\mathcal{L}_2 = -\frac{1}{4}F_{\mu\nu}F^{\mu\nu} + \frac{1}{4}f^2\langle\nabla_\mu\Sigma\nabla^\mu\Sigma^\dagger\rangle + \frac{1}{4}f^2\langle\chi^\dagger\Sigma + \Sigma^\dagger\chi\rangle + C\langle Q\Sigma Q\Sigma^\dagger\rangle + \mathcal{L}_{\rm gf} + \mathcal{L}_{\rm ghost}, \tag{34}$$

where the first term is the kinetic term for the photons. The covariant derivatives are

$$\nabla_\mu\Sigma = \partial_\mu\Sigma + i[A_\mu Q, \Sigma], \tag{35}$$

$$\nabla_\mu\Sigma^\dagger = \partial_\mu\Sigma^\dagger + i[A_\mu Q, \Sigma^\dagger]. \tag{36}$$

where the charge matrix of the quarks is

$$Q = \frac{1}{2}e\left(\lambda_3 + \frac{1}{\sqrt{3}}\lambda_8\right). \tag{37}$$

Since our calculations involve the dynamical gauge field A_μ, we need to fix the gauge. In the class of covariant gauges, the gauge-fixing term is

$$\mathcal{L}_{\rm gf} = \frac{1}{2\xi}(\partial_\mu A^\mu)^2, \tag{38}$$

where ξ is the gauge-fixing parameter. The corresponding ghost term is

$$\mathcal{L}_{\text{ghost}} = \frac{1}{2}\partial_\mu \bar{c}\partial^\mu c. \tag{39}$$

The ghost completely decouples from the rest of the Lagrangian. In a general covariant gauge, the Euclidean space photon and ghost propagators are

$$\Delta_{\mu\nu}(P) = \frac{1}{P^2}\left(\delta_{\mu\nu} - (1-\xi)\frac{P_\mu P_\nu}{P^2}\right), \tag{40}$$

$$\Delta_{\text{ghost}}(P) = \frac{1}{P^2}. \tag{41}$$

At $\mathcal{O}(p^4)$, the partial derivatives are also replaced by covariant derivatives in Eq. (17). The $\mathcal{O}(p^4)$ chiral Lagrangian has an additional 17 terms whose coefficients were computed in the Feynman gauge, $\xi = 1$ [9–12]. Generally, the coefficients of the operators depend on the gauge, an explicit example is given in Ref. [31]. Some of the operators have two powers of e and two derivatives, or two powers of e with one power of the quark mass, or four powers of e. The 14 operators required are

$$\begin{aligned}\mathcal{L}_4^Q = {} & K_1 f^2\langle\nabla_\mu\Sigma^\dagger\nabla^\mu\Sigma\rangle\langle Q^2\rangle + K_2 f^2\langle\nabla_\mu\Sigma^\dagger\nabla^\mu\Sigma\rangle\langle Q\Sigma Q\Sigma^\dagger\rangle + K_3 f^2(\langle\nabla_\mu\Sigma^\dagger Q\Sigma\rangle\langle\nabla^\mu\Sigma^\dagger Q\Sigma\rangle + \langle\nabla_\mu\Sigma Q\Sigma^\dagger\rangle\langle\nabla^\mu\Sigma Q\Sigma^\dagger\rangle)\\ & + K_4 f^2\langle\nabla_\mu\Sigma^\dagger Q\Sigma\rangle\langle\nabla^\mu\Sigma Q\Sigma^\dagger\rangle + K_5 f^2\langle(\nabla_\mu\Sigma^\dagger\nabla^\mu\Sigma + \nabla_\mu\Sigma\nabla^\mu\Sigma^\dagger)Q^2\rangle + K_6 f^2\langle\nabla_\mu\Sigma^\dagger\nabla^\mu\Sigma Q\Sigma^\dagger Q\Sigma + \nabla_\mu\Sigma\nabla^\mu\Sigma^\dagger Q\Sigma Q\Sigma^\dagger\rangle\\ & + K_7 f^2\langle\chi^\dagger\Sigma + \Sigma^\dagger\chi\rangle\langle Q^2\rangle + K_8 f^2\langle\chi^\dagger\Sigma + \Sigma^\dagger\chi\rangle\langle Q\Sigma Q\Sigma^\dagger\rangle + K_9 f^2\langle(\chi^\dagger\Sigma + \Sigma^\dagger\chi + \chi\Sigma^\dagger + \Sigma\chi^\dagger)Q^2\rangle\\ & + K_{10} f^2\langle(\chi^\dagger\Sigma + \Sigma^\dagger\chi)Q\Sigma^\dagger Q\Sigma + (\chi\Sigma^\dagger + \Sigma\chi^\dagger)Q\Sigma Q\Sigma^\dagger\rangle + K_{11} f^2\langle(\chi^\dagger\Sigma - \Sigma^\dagger\chi)Q\Sigma^\dagger Q\Sigma + (\chi\Sigma^\dagger - \Sigma\chi^\dagger)Q\Sigma Q\Sigma^\dagger\rangle\\ & + K_{15} f^4\langle Q\Sigma Q\Sigma^\dagger\rangle^2 + K_{16} f^4\langle Q\Sigma Q\Sigma^\dagger\rangle\langle Q^2\rangle + K_{17} f^4\langle Q^2\rangle^2,\end{aligned} \tag{42}$$

where K_1–K_{17} are constants. The last operator is a contact term. The relation between the bare and renormalized couplings is

$$K_i = K_i^r - \frac{\Lambda^{-2\epsilon}\Sigma_i}{2(4\pi)^2}\left[\frac{1}{\epsilon} + 1\right], \tag{43}$$

where the constants Σ_i are

$$\Sigma_1 = \frac{3}{4}, \qquad \Sigma_2 = Z, \tag{44}$$

$$\Sigma_3 = -\frac{3}{4}, \qquad \Sigma_4 = 2Z, \tag{45}$$

$$\Sigma_5 = -\frac{9}{4}, \qquad \Sigma_6 = \frac{3}{2}Z, \tag{46}$$

$$\Sigma_7 = 0, \qquad \Sigma_8 = Z, \tag{47}$$

$$\Sigma_9 = -\frac{1}{4}, \qquad \Sigma_{10} = \frac{1}{4} + \frac{3}{2}Z, \tag{48}$$

$$\Sigma_{11} = \frac{1}{8}, \qquad \Sigma_{15} = \frac{3}{2} + 3Z + 14Z^2, \tag{49}$$

$$\Sigma_{16} = -3 - \frac{3}{2}Z - Z^2, \qquad \Sigma_{17} = \frac{3}{2} - \frac{3}{2}Z + 5Z^2, \tag{50}$$

and $Z = \frac{C}{f^4}$. The running of K_i^r is given by the solution to the renormalization group equation

$$\Lambda\frac{dK_i^r}{d\Lambda} = -\frac{\Sigma_i}{(4\pi)^2}. \tag{51}$$

Note that $\Sigma_7 = 0$ which implies that K_7 does not run and we write $K_7 = K_7^r$.

The charged mesons receive a contribution to the tree-level mass from the term $C\langle Q\Sigma Q\Sigma^\dagger\rangle$ in the Lagrangian Eq. (34). Expanding this term to second order in the fields, we find

$$\begin{aligned}\delta\mathcal{L}_2^{\text{quadratic}} &= -\frac{Ce^2}{f^2}[\phi_1^2 + \phi_2^2 + \phi_4^2 + \phi_2^5]\\ &= -2\frac{Ce^2}{f^2}[\pi^+\pi^- + K^+K^-],\end{aligned} \tag{52}$$

and therefore

$$m_{\pi^\pm,0}^2 = B_0(m_u + m_d) + 2\frac{Ce^2}{f^2}, \tag{53}$$

$$m_{K^\pm,0}^2 = B_0(m_u + m_s) + 2\frac{Ce^2}{f^2}. \tag{54}$$

The new term which is of purely electromagnetic origin gives rise to the mass splitting of the neutral and charged mesons that is nonzero in the chiral limit.

We also need the Lagrangian to fourth order in the fields. The new terms are coming from the covariant derivative and from the term $C\langle Q\Sigma Q\Sigma^\dagger\rangle$. We find

$$\mathcal{L}_2^{Q,\text{quartic}} = \frac{Ce^2}{6f^4}[8(\pi^+\pi^-)^2 + 4\pi^+\pi^-(\pi^0)^2 + 16\pi^+\pi^-K^+K^- + 2\pi^+\pi^-K^0\bar{K}^0 + (\pi^0)^2K^+K^- + 8(K^+K^-)^2 + 2K^+K^-K^0\bar{K}^0 + 3K^+K^-\eta^2] + ie(\pi^+\partial_\mu\pi^- - \pi^-\partial_\mu\pi^+)A^\mu + ie(K^+\partial_\mu K^- - K^-\partial_\mu K^+)A^\mu + e^2(\pi^+\pi^- + K^+K^-)A_\mu A^\mu. \tag{55}$$

The one-loop counterterms are found by expanding $\mathcal{L}_4^Q$ in Eq. (42) to second order in the fields. One finds

$$\begin{aligned}\mathcal{L}_4^{Q,\text{quadratic}} =& \frac{4}{3}e^2(K_1+K_2)[\partial_\mu\pi^0\partial^\mu\pi^0 + 2\partial_\mu\pi^+\partial^\mu\pi^- + 2\partial_\mu K^+\partial^\mu K^- + 2\partial_\mu K^0\partial^\mu\bar{K}^0 + \partial_\mu\eta\partial^\mu\eta] - \frac{1}{3}e^2(2K_3 - K_4)\\ &\times[3\partial_\mu\pi^0\partial^\mu\pi^0 + \partial_\mu\eta\partial^\mu\eta] + \frac{2}{9}e^2(K_5+K_6)[5\partial_\mu\pi^0\partial^\mu\pi^0 + 10\partial_\mu\pi^+\partial^\mu\pi^- + 10\partial_\mu K^+\partial^\mu K^- + 4\partial_\mu K^0\partial^\mu\bar{K}^0 + 3\partial_\mu\eta\partial^\mu\eta]\\ &- \frac{4}{3}e^2(K_7+K_8)[m_{\pi,0}^2(\pi^0)^2 + 2m_{\pi,0}^2\pi^+\pi^- + 2m_{K,0}^2(K^+K^- + K^0\bar{K}^0) + m_{\eta,0}^2\eta^2] - 4e^2K_8(m_{\pi,0}^2 + 2m_{K,0}^2)\\ &\times(\pi^+\pi^- + K^+K^-) - \frac{2e^2K_9}{27}[m_{\pi,0}^2(30\pi^+\pi^- + 15(\pi^0)^2 + 18K^+K^- + \eta^2) + m_{K,0}^2(12K^+K^- + 12K^0\bar{K}^0 + 8\eta^2)]\\ &- \frac{2e^2K_{10}}{27}[m_{\pi,0}^2(138\pi^+\pi^- + 15(\pi^0)^2 + 18K^+K^- + \eta^2) + m_{K,0}^2(120K^+K^- + 12K^0\bar{K}^0 + 8\eta^2)]\\ &- 8e^2K_{11}(m_{\pi,0}^2\pi^+\pi^- + m_{K,0}^2K^+K^-) - \frac{8}{3}f^2e^4K_{15}(\pi^+\pi^- + K^+K^-) - \frac{4}{3}f^2e^4K_{16}(\pi^+\pi^- + K^+K^-).\end{aligned} \tag{56}$$

Again there will be static terms from $\mathcal{L}_6^Q$ contributing to the renormalization of the vacuum energy and we will not need them.

V. PRESSURE REVISITED

In this section, we calculate the pressure through $\mathcal{O}(p^6)$ including electromagnetic interactions. Since the neutral and charged mesons are no longer degenerate in masses, we must express the pressure in terms of all the five different meson masses. As mentioned before, the chiral Lagrangian including virtual photons is known only to $\mathcal{O}(p^4)$. It therefore not possible to renormalize the vacuum energy through $\mathcal{O}(p^6)$, but it is possible to renormalize the finite-temperature part since the counterterms at the relevant order are given by the $\mathcal{O}(p^4)$ Lagrangian.

A. $\mathcal{O}(p^4)$

Again the temperature-independent $\mathcal{O}(p^2)$-term is omitted. The mesonic one-loop contribution to the pressure is the same as before, except that the charged masses have changed according to Eqs. (53) and (54). In addition, there is a contribution from the massless photons, giving

$$\mathcal{P}_1 = \frac{1}{2}I_0'(m_{\pi,0}^2) + I_0'(m_{\pi^\pm,0}^2) + I_0'(m_{K^\pm,0}^2) + I_0'(m_{K,0}^2) + \frac{1}{2}I_0'(m_{\eta,0}^2) + \frac{1}{2}(d-1)I_0'(0), \tag{57}$$

where $d = 3 - 2\epsilon$. Omitting the temperature-independent divergent terms yields in the limit $\epsilon \to 0$

$$\mathcal{P}_1 = \frac{T^4}{(4\pi)^2}\left[\frac{1}{2}J_0(\beta m_{\pi,0}) + J_0(\beta m_{\pi^\pm,0}) + J_0(\beta m_{K,0}) + J_0(\beta m_{K^\pm,0}) + \frac{1}{2}J_0(\beta m_{\eta,0}) + J_0(0)\right], \tag{58}$$

where $J_0(0) = \frac{16\pi^4}{45}$.

B. $\mathcal{O}(p^6)$

The two-loop diagrams are those given in the previous section as well as a number of new ones coming from the interaction terms in Eq. (55). The second group of diagrams are shown in Fig. 3. These are the only diagrams involving the photon propagator. We note in passing that the individual diagrams are gauge-fixing dependent, but the sum is independent of ξ in covariant gauge. The same result is obtained in the Coulomb gauge with gauge parameter ξ.

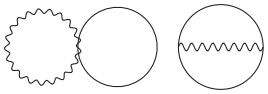

FIG. 3. Feynman graphs contributing to the pressure at next-to-next-to leading order. Solid lines represent a charged meson and wavy lines represent a photon. The setting-sun diagram is shown to the right.

The expression for the diagrams in Fig. 1 is

$$\begin{aligned}\mathcal{P}_2^a = &-\frac{m_{\pi,0}^2}{f^2}\left[-\frac{1}{8}I_1^2(m_{\pi,0}^2)+\frac{1}{6}I_1(m_{\pi^\pm,0}^2)I_1(m_{\pi,0}^2)-\frac{1}{3}I_1^2(m_{\pi^\pm,0}^2)-\frac{1}{6}I_1(m_{\pi^\pm,0}^2)I_1(m_{K,0}^2)\right.\\&\left.-\frac{1}{6}I_1(m_{\pi^\pm,0}^2)I_1(m_{K^\pm,0}^2)-\frac{1}{12}I_1(m_{\pi,0}^2)I_1(m_{\eta,0}^2)-\frac{1}{6}I_1(m_{\pi^\pm,0}^2)I_1(m_{\eta,0}^2)+\frac{7}{72}I_1^2(m_{\eta,0}^2)\right]\\&-\frac{m_{\pi^\pm,0}^2}{f^2}\left[\frac{1}{3}I_1(m_{\pi^\pm,0}^2)I_1(m_{\pi,0}^2)+\frac{1}{3}I_1^2(m_{\pi^\pm,0}^2)+\frac{1}{6}I_1(m_{\pi^\pm,0}^2)I_1(m_{K,0}^2)+\frac{1}{6}I_1(m_{\pi^\pm,0}^2)I_1(m_{K^\pm,0}^2)\right]\\&-\frac{m_{K,0}^2}{f^2}\left[-\frac{1}{3}I_1^2(m_{K^\pm,0}^2)-\frac{1}{12}I_1(m_{\pi,0}^2)I_1(m_{K^\pm,0}^2)-\frac{1}{6}I_1(m_{\pi^\pm,0}^2)I_1(m_{K^\pm,0}^2)-\frac{1}{6}I_1(m_{K,0}^2)I_1(m_{K^\pm,0}^2)\right.\\&\left.+\frac{1}{3}I_1(m_{K^0,0}^2)I_1(m_{\eta,0}^2)+\frac{1}{12}I_1(m_{K^\pm,0}^2)I_1(m_{\eta,0}^2)-\frac{2}{9}I_1^2(m_{\eta,0}^2)\right]-\frac{m_{K^\pm,0}^2}{f^2}\left[\frac{1}{3}I_1^2(m_{K^\pm,0}^2)+\frac{1}{12}I_1(m_{\pi,0}^2)I_1(m_{K^\pm,0}^2)\right.\\&\left.+\frac{1}{6}I_1(m_{\pi^\pm,0}^2)I_1(m_{K^\pm,0}^2)+\frac{1}{6}I_1(m_{K,0}^2)I_1(m_{K^\pm,0}^2)+\frac{1}{4}I_1(m_{K^\pm,0}^2)I_1(m_{\eta,0}^2)\right],\end{aligned}\tag{59}$$

where the charged masses are given by Eqs. (53) and (54). Setting $e=0$, i.e., for degenerate meson masses, Eq. (59) reduces to Eq. (28), as it should.

The first set of one-loop graphs with insertions is shown in Fig. 2. Their expression is

$$\begin{aligned}\mathcal{P}_2^b = &\frac{4L_4}{f^2}(m_{\pi,0}^2+2m_{K,0}^2)[2m_{\pi^\pm,0}^2I_1(m_{\pi^\pm,0}^2)+m_{\pi,0}^2I_1(m_{\pi,0}^2)+2m_{K^\pm,0}^2I_1(m_{K^\pm,0}^2)+2m_{K,0}^2I_1(m_{K,0}^2)+m_{\eta,0}^2I_1(m_{\eta,0}^2)]\\&+\frac{4L_5}{f^2}[m_{\pi,0}^2(2m_{\pi^\pm,0}^2I_1(m_{\pi^\pm,0}^2)+m_{\pi,0}^2I_1(m_{\pi,0}^2))+2m_{K,0}^2(m_{K^\pm,0}^2I_1(m_{K^\pm,0}^2)+m_{K,0}^2I_1(m_{K,0}^2))+m_{\eta,0}^4I_1(m_{\eta,0}^2)]\\&-\frac{8L_6}{f^2}(m_{\pi,0}^2+2m_{K,0}^2)[m_{\pi,0}^2(2I_1(m_{\pi^\pm,0}^2)+I_1(m_{\pi,0}^2))+2m_{K,0}^2(I_1(m_{K^\pm,0}^2)+I_1(m_{K,0}^2))+m_{\eta,0}^2I_1(m_{\eta,0}^2)]\\&-\frac{64L_7}{3f^2}(m_{\pi,0}^2-m_{K,0}^2)^2I_1(m_{\eta,0}^2)-\frac{16L_8}{f^2}\left[m_{\pi,0}^4\left(I_1(m_{\pi^\pm,0}^2)+\frac{1}{2}I_1(m_{\pi,0}^2)\right)+m_{K,0}^4(I_1(m_{K^\pm,0}^2)+I_1(m_{K,0}^2))\right.\\&\left.+\frac{1}{3}\left(4m_{K,0}^4-4m_{\pi,0}^2m_{K,0}^2+\frac{3}{2}m_{\pi,0}^4\right)I_1(m_{\eta,0}^2)\right].\end{aligned}\tag{60}$$

The expression for diagrams arising from the interactions in Eq. (55) and shown in Fig. 3 is

$$\begin{aligned}\mathcal{P}_2^c = &-(d-1)e^2I_1(m_{\pi^\pm,0}^2)I_1(0)-\frac{1}{2}e^2I_1^2(m_{\pi^\pm,0}^2)-2e^2m_{\pi^\pm,0}^2I_{\rm sun}(m_{\pi^\pm,0}^2)-(d-1)e^2I_1(m_{K^\pm,0}^2)I_1(0)\\&-\frac{1}{2}e^2I_1^2(m_{K^\pm,0}^2)-2e^2m_{K^\pm,0}^2I_{\rm sun}(m_{K^\pm,0}^2)+\frac{Ce^2}{6f^4}[4I_1(m_{\pi,0}^2)I_1(m_{\pi^\pm,0}^2)+16I_1^2(m_{\pi^\pm,0}^2)+16I_1(m_{\pi^\pm,0}^2)I_1(m_{K^\pm,0}^2)\\&+I_1(m_{\pi,0}^2)I_1(m_{K^\pm,0}^2)+2I_1(m_{\pi^\pm,0}^2)I_1(m_{K,0}^2)+16I_1^2(m_{K^\pm,0}^2)+2I_1(m_{K^\pm,0}^2)I_1(m_{K,0}^2)+3I_1(m_{K^\pm,0}^2)I_1(m_{\eta,0}^2)],\end{aligned}\tag{61}$$

where $d=3-2\epsilon$ and $I_{\rm sun}(m^2)$ is defined in Eq. (B1). $I_{\rm sun}(m^2)$ is evaluated in Appendix B. Finally, the expression for the diagrams arising from Eq. (56) are given by

$$\mathcal{P}_2^d = \frac{4}{3}e^2(K_1+K_2)[m_{\pi,0}^2 I_1(m_{\pi,0}^2)+2m_{\pi^\pm,0}^2 I_1(m_{\pi^\pm,0}^2)+2m_{K,0}^2 I_1(m_{K,0}^2)+2m_{K^\pm,0}^2 I_1(m_{K^\pm,0}^2)+m_{\eta,0}^2 I_1(m_{\eta,0}^2)]$$
$$+\frac{1}{3}e^2(-2K_3+K_4)[3m_{\pi,0}^2 I_1^2(m_{\pi,0})+m_{\eta,0}^2 I_1^2(m_{\eta,0})]+\frac{2}{9}e^2(K_5+K_6)[5m_{\pi,0}^2 I_1(m_{\pi,0}^2)+10m_{\pi^\pm,0}^2 I_1(m_{\pi^\pm,0}^2)$$
$$+10m_{K^\pm,0}^2 I_1(m_{K^\pm,0}^2)+4m_{K,0}^2 I_1(m_{K,0}^2)+3m_{\eta,0}^2 I_1(m_{\eta,0}^2)]-\frac{4}{3}e^2(K_7+K_8)[m_{\pi,0}^2(I_1(m_{\pi,0}^2)+2I_1(m_{\pi^\pm,0}^2))$$
$$+2m_{K,0}^2(I_1(m_{K^\pm,0}^2)+I_1(m_{K,0}^2))+m_{\eta,0}^2 I_1(m_{\eta,0}^2)]-4e^2K_8(m_{\pi,0}^2+2m_{K,0}^2)[I_1(m_{\pi^\pm,0}^2)+I_1(m_{K^\pm,0}^2)]$$
$$-\frac{2e^2K_9}{27}[m_{\pi,0}^2(30I_1(m_{\pi^\pm,0}^2)+15I_1(m_{\pi,0}^2)+18I_1(m_{K^\pm,0}^2)+I_1(m_{\eta,0}^2))+m_{K,0}^2(12I_1(m_{K^\pm,0}^2)+12I_1(m_{K,0}^2)$$
$$+8I_1(m_{\eta,0}^2))]-\frac{2e^2K_{10}}{27}[m_{\pi,0}^2(138I_1(m_{\pi^\pm,0}^2)+15I_1(m_{\pi,0}^2)+18I_1(m_{K^\pm,0}^2)+I_1(m_{\eta,0}^2))+m_{K,0}^2(120I_1(m_{K^\pm,0}^2)$$
$$+12I_1(m_{K,0}^2)+8I_1(m_{\eta,0}^2))]-8e^2K_{11}[m_{\pi,0}^2 I_1(m_{\pi^\pm,0}^2)+m_{K,0}^2 I_1(m_{K^\pm,0}^2)]. \tag{62}$$

The complete result for the pressure is then given by the sum of Eqs. (58)–(62). Again we can absorb the terms that involve the low-energy constants by replacing the bare meson masses with their one-loop expression. The final result is

$$\mathcal{P}_{0+1+2}=\frac{T^4}{(4\pi)^2}\left[\frac{1}{2}J_0(\beta m_{\pi^0})+J_0(\beta m_{\pi^\pm})+J_0(\beta m_{K^0})+J_0(\beta m_{K^\pm})+\frac{1}{2}J_0(\beta m_\eta)+J_0(0)\right]$$
$$-\frac{m_{\pi,0}^2T^4}{(4\pi)^4f^2}\left[\frac{1}{2}J_1(\beta m_{\pi^\pm,0})J_1(\beta m_{\pi,0})-\frac{1}{8}J_1^2(\beta m_{\pi,0})-\frac{1}{12}J_1(\beta m_{\pi,0})J_1(\beta m_{\eta,0})-\frac{1}{6}J_1(\beta m_{\pi^\pm,0})J_1(\beta m_{\eta,0})\right.$$
$$\left.+\frac{7}{72}J_1^2(\beta m_{\eta,0})\right]-\frac{m_{K,0}^2T^4}{(4\pi)^4f^2}\left[\frac{1}{3}J_1(\beta m_{K,0})J_1(\beta m_{\eta,0})+\frac{1}{3}J_1(\beta m_{K^\pm,0})J_1(\beta m_{\eta,0})-\frac{2}{9}J_1^2(\beta m_{\eta,0})\right]$$
$$-\frac{e^2T^4}{(4\pi)^4}\left[2J_1(\beta m_{\pi^\pm,0})J_1(0)+\frac{1}{2}J_1^2(\beta m_{\pi^\pm,0})+2J_1(\beta m_{K^\pm,0})J_1(0)+\frac{1}{2}J_1^2(\beta m_{K^\pm,0})\right]-2m_{\pi^\pm,0}^2e^2I_{\rm sun}^{(2)}(m_{\pi^\pm,0}^2)$$
$$-2m_{K^\pm,0}^2e^2I_{\rm sun}^{(2)}(m_{K^\pm,0}^2)+\frac{Ce^2T^4}{(4\pi)^4f^4}[2J_1^2(\beta m_{\pi^\pm,0})+2J_1(\beta m_{\pi^\pm,0})J_1(\beta m_{K^\pm,0})+2J_1^2(\beta m_{K^\pm,0})]. \tag{63}$$

where $I_{\rm sun}^{(2)}(m^2)$ is defined in Eq. (B16) and we note that $J_1(0)=\frac{4\pi^2}{3}$.

VI. QUARK CONDENSATES

In the vacuum, the light and s-quark condensates are defined as

$$\langle\bar{u}u\rangle_0=\frac{\partial V}{\partial m_u}, \tag{64}$$

$$\langle\bar{d}d\rangle_0=\frac{\partial V}{\partial m_d}, \tag{65}$$

$$\langle\bar{s}s\rangle_0=\frac{\partial V}{\partial m_s}, \tag{66}$$

where V is the vacuum energy density. By introducing the sum $m=\frac{1}{2}(m_u+m_d)$ and difference $\Delta m=\frac{1}{2}(m_u-m_d)$ of the light quark masses, we calculate the sum and difference of the light quark condensates as

$$\langle\bar{u}u\rangle_0+\langle\bar{d}d\rangle_0=\langle\bar{q}q\rangle_0=\frac{\partial V}{\partial m}, \tag{67}$$

$$\langle\bar{u}u\rangle_0-\langle\bar{d}d\rangle_0=\frac{\partial V}{\partial\Delta m}. \tag{68}$$

At finite temperature, we replace V by $V-\mathcal{P}$ [15] and we therefore have

$$\langle\bar{q}q\rangle=\langle\bar{q}q\rangle_0\left[1+\sum_a\frac{c_a}{f^2}\frac{\partial\mathcal{P}}{\partial m_a^2}\right], \tag{69}$$

$$\langle\bar{s}s\rangle=\langle\bar{s}s\rangle_0\left[1+\sum_a\frac{c_{sa}}{f^2}\frac{\partial\mathcal{P}}{\partial m_a^2}\right], \tag{70}$$

where the sum is over the eight mesons and the coefficients are

$$c_a=-f^2\frac{\partial m_a^2}{\partial m}\langle\bar{q}q\rangle_0^{-1}, \tag{71}$$

$$c_{sa} = -f^2 \frac{\partial m_a^2}{\partial m_s} \langle \bar{s}s \rangle_0^{-1}. \tag{72}$$

The expressions for the coefficients are obtained by using the results for the condensates at $T = 0$ given by (C5) and (C6) and the meson masses listed in Eqs. (D1)–(D8).

VII. HADRON RESONANCE GAS MODEL

In the HRG model, one approximates the partition function of the system by the partition function of a gas of noninteracting hadrons and resonances. The pressure $\mathcal{P}$ is therefore given by the sum of independent contributions $\mathcal{P}_h$ coming from the different species,

$$\begin{aligned}\mathcal{P} &= \sum_h \mathcal{P}_h \\ &= \mp \frac{8T}{(4\pi)^2} \sum_h d_h (2s+1) \int_0^\infty dp\, p^2 \log\left[1 \mp e^{-\beta\sqrt{p^2+m_h^2}}\right],\end{aligned} \tag{73}$$

where d_h is the multiplicity, s is the spin, m_h is the hadron mass, and the upper (lower) sign is for mesons (baryons). The lightest hadrons we include in the sum are shown in Table I. In the numerical work, the used HRG model includes more than 200 known mesons and baryons below 2.5 GeV in Particle Data Group [32]. As known from Ref. [18], it is reasonable to add those known resonances. Of course, it includes those broad light flavor mesons e.g. $f_0(500)$, $f_0(1370)$, and $K_0^*(700)$ where we take the central values of the estimated masses.

We also need the expressions for the condensates in the HRG model. They are given by

$$\begin{aligned}\langle \bar{q}q \rangle &= \langle \bar{q}q \rangle_0 - \frac{\partial \mathcal{P}}{\partial m} \\ &= \langle \bar{q}q \rangle_0 + \sum_h n_h(T) \frac{\partial m_h}{\partial m},\end{aligned} \tag{74}$$

TABLE I. Lightest hadrons included in the hadron resonance gas model.

Hadron	m(MeV)	s	d_h	Hadron	m(MeV)	s	d_h
$\pi^\pm$	139.57	0	2	p	938.27	1/2	2
π^0	134.98	0	1	n	939.57	1/2	2
$K^\pm$	493.68	0	2	η'	957.78	0	1
$K^0/\bar{K}^0$	497.61	0	2	f_0	990 ± 20	0	1
η	547.86	0	1	a_0	980 ± 20	1	1
$\rho^\pm$	775.26	1	2	ϕ	1019.46	1	1
ρ	775.26	1	1	Λ	1115.68	1/2	1
ω	782.66	1	1	h_1	1166 ± 6	1	1
$K_*^\pm$	891.67	1	2	$\Sigma^\pm$	1189.37	1/2	2
K_*^0	895.55	1	2	Σ^0	1192.64	1/2	1

$$\begin{aligned}\langle \bar{s}s \rangle &= \langle \bar{s}s \rangle_0 - \frac{\partial \mathcal{P}}{\partial m_s} \\ &= \langle \bar{s}s \rangle_0 + \sum_h n_h(T) \frac{\partial m_h}{\partial m_s},\end{aligned} \tag{75}$$

$$\tag{76}$$

where the temperature dependent density of hadrons is

$$n_h(T) = \frac{8 d_h (2s+1)}{(4\pi)^2} \int_0^\infty dp\, \frac{m_h p^2}{\sqrt{p^2+m_h^2}} \frac{1}{e^{\beta\sqrt{p^2+m_h^2}} \mp 1}. \tag{77}$$

The derivatives of the hadrons masses with respect to the light quark mass m and the strange quark mass m_s can be written as [18]

$$\frac{\partial m_h}{\partial m} = 2B_0 \frac{\sigma_{\pi,h}}{m_{\pi^0}^2}, \tag{78}$$

$$\frac{\partial m_h}{\partial m_s} = \frac{\sigma_{s,h}}{m_s} = \frac{\sigma_{s,h}}{m_{K,0}^2} \frac{B_0(m+m_s)}{m_s}. \tag{79}$$

The sigma terms for the fundamental states are taken from [33]. It is difficult to calculate the sigma terms for each particle, but we follow Ref. [18] and assume that all hadrons have the same sigma term as their fundamental state.

VIII. NUMERICAL RESULTS AND DISCUSSION

In this section, we present and discuss our numerical results. As input we will use the physical meson masses and the pion decay constant taken from the Particle Data Group [32]

$$m_{\pi^0} = 134.98 \text{ MeV}, \tag{80}$$

$$m_{\pi^\pm} = 139.57 \text{ MeV}, \tag{81}$$

$$m_{K^\pm} = 493.68 \text{ MeV}, \tag{82}$$

$$m_{K^0} = 497.61 \text{ MeV}, \tag{83}$$

$$m_\eta = 547.86 \text{ MeV}, \tag{84}$$

$$f_\pi = 92.07 \text{ MeV}. \tag{85}$$

The numerical values of the low-energy constants that we need are [7,34], where Ref. [7] includes $L_4^r - L_8^r$ and H_2^r is taken from Ref. [34],

$$L_4^r = (0.0 \pm 0.3) \times 10^{-3}, \tag{86}$$

$$L_5^r = (1.2 \pm 0.1) \times 10^{-3}, \tag{87}$$

$$L_6^r = (0.0 \pm 0.4) \times 10^{-3}, \tag{88}$$

$$L_7^r = (-0.3 \pm 0.2) \times 10^{-3}, \tag{89}$$

$$L_8^r = (0.5 \pm 0.2) \times 10^{-3}, \tag{90}$$

$$H_2^r = (-3.4 \pm 1.5) \times 10^{-3}. \tag{91}$$

These couplings are at the scale of the ρ mass, $\Lambda = 775.26$ MeV.

Including electromagnetic interactions, we need a number of additional couplings. The electromagnetic coupling is [32]

$$e^2 = 0.092. \tag{92}$$

The numerical value of the constant C has been estimated by Urech [9]. Its value is

$$C = 61.1 \times 10^{-6}(\text{GeV})^4. \tag{93}$$

At tree level, this gives rise to a mass splitting between the neutral and charged pion of approximately 4.8 MeV, which is very close the experimental value of 4.6 MeV. Finally, we need [7,35,36]

$$K_1^r = -2.7 \times 10^{-3}, \tag{94}$$

$$K_2^r = 0.7 \times 10^{-3}, \tag{95}$$

$$K_3^r = 2.7 \times 10^{-3}, \tag{96}$$

$$K_4^r = 1.4 \times 10^{-3}, \tag{97}$$

$$K_5^r = 11.6 \times 10^{-3}, \tag{98}$$

$$K_6^r = 2.8 \times 10^{-3}, \tag{99}$$

$$K_7^r = 0 \times 10^{-3}, \tag{100}$$

$$K_8^r = 0 \times 10^{-3}, \tag{101}$$

$$K_9^r = -1.3 \times 10^{-3}, \tag{102}$$

$$K_{10}^r = 4 \times 10^{-3}, \tag{103}$$

$$K_{11}^r = 1.3 \times 10^{-3}, \tag{104}$$

where all the K_i^r are assigned a conservative 100% uncertainty [35]. The low-energy constants $K_1^r - K_8^r$ and K_{11}^r can be found in Ref. [7], K_9^r and K_{10}^r are from Ref. [36].

If we ignore electromagnetic interactions, the charged pion is degenerate with the neutral pion, and the charged kaon is degenerate with the neutral kaon. In this case, we use the experimental values for the masses of the neutral mesons as well as f_π. Using these values together with the low-energy constants, Eqs. (D1), (D2), and (D9) (here with $e = 0$) give us the tree-level values for $m_{\pi,0}$, $m_{K,0}$, and f. The tree-level value of the eta mass is then given by the relation $m_{\eta,0}^2 = \frac{1}{3}(4m_{K,0}^2 - m_{\pi,0}^2)$. The bare values we find are

$$m_{\pi,0} = 135.52 \text{ MeV}, \tag{105}$$

$$m_{K,0} = 536.72 \text{ MeV}, \tag{106}$$

$$m_{\eta,0} = 614.79 \text{ MeV}, \tag{107}$$

$$f = 76.93 \text{ MeV}. \tag{108}$$

Adding electromagnetic effects, we obtain

$$m_{\pi,0} = 135.97 \text{ MeV}, \tag{109}$$

$$m_{\pi^\pm,0} = 137.11 \text{ MeV}, \tag{110}$$

$$m_{K^\pm,0} = 531.85 \text{ MeV}, \tag{111}$$

$$m_{K,0} = 537.14 \text{ MeV}, \tag{112}$$

$$m_{\eta,0} = 615.25 \text{ MeV}, \tag{113}$$

$$f = 76.69 \text{ MeV}. \tag{114}$$

In both cases, we see that renormalization effects are modest, except for the pion-decay constant.

In Fig. 4, we show some of the individual contributions to the pressure in the HRG model in units of 10^{-4} GeV^4 as a function of temperature in MeV. This is essentially the same

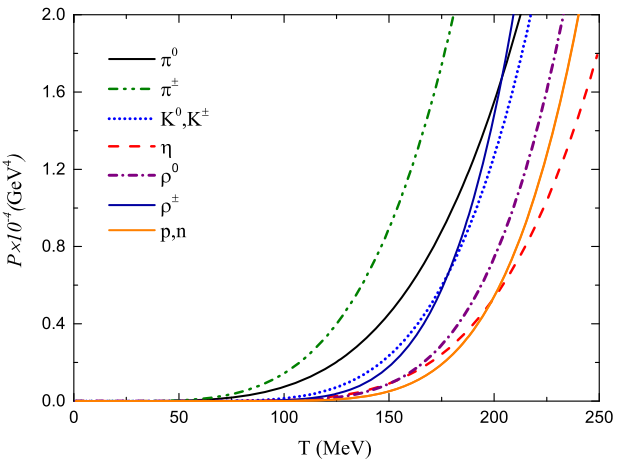

FIG. 4. Individual contributions to the pressure in the HRG model as a function of the temperature in MeV. See main text for details.

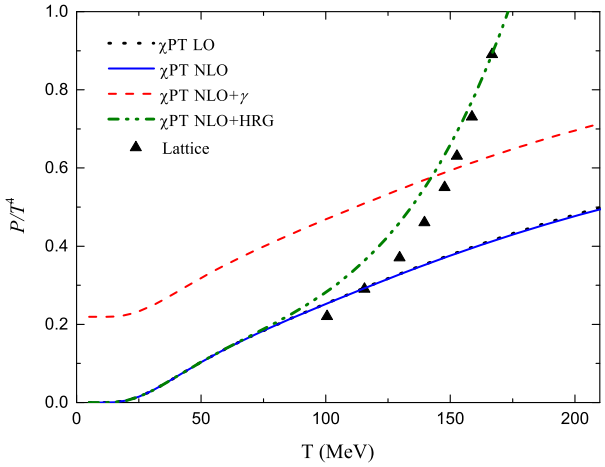

FIG. 5. Pressure normalized by T^4 as a function of the temperature in MeV. See main text for details.

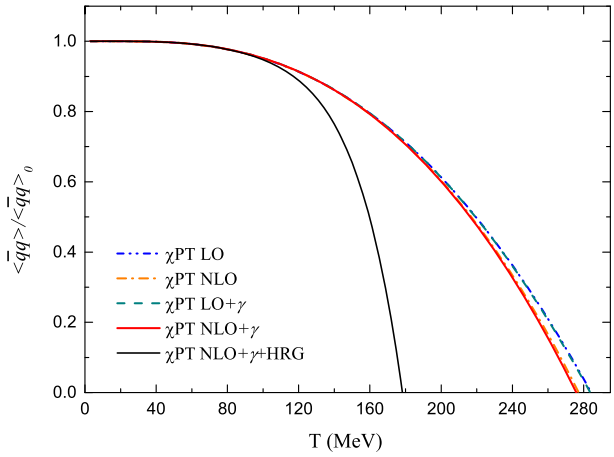

FIG. 6. Normalized light quark condensate $\langle\bar{q}q\rangle/\langle\bar{q}q\rangle_0$ as a function of the temperature in MeV. See main text for details.

as Fig. 2 of Ref. [37]. As expected, at any given temperature, the lightest states contribute more to the total pressure than the heavier states. Up to approximately 100 MeV, only the pions contribute significantly. From 120 to 130 MeV onwards, heavier states that are not included in three-flavor χPT start to contribute significantly.

In Fig. 5, we show the pressure $\mathcal{P}$ normalized to T^4 in various approximations. The dotted line is the $\mathcal{O}(p^2)$ result in χPT, while the blue line is $\mathcal{O}(p^4)$ result. The red dashed line is the $\mathcal{O}(p^4)$ result including electromagnetic effects. The green line shows the resulting normalized pressure combining χPT and the hadron resonance gas model. Doing this, the eight mesons in three-flavor χPT are excluded from the sum in Eq. (73) so we do not count degrees of freedom twice. The black triangles are the lattice results taken from Ref. [18]. For low temperatures, the contribution to the pressure from the massive states is Boltzmann suppressed. This implies that the normalized pressure vanishes, except for the case where the contribution from the photons is included. The normalized pressure in the limit $T \to 0$ is therefore $2 \times \frac{\pi^2}{90} = 0.22$. The difference between the red and the blue line is fairly constant over the temperature range shown, indicating that electromagnetic interactions contribute relatively little to the total pressure. The green and blue lines are essentially on top of each other until a temperature of approximately 90 MeV, where they start to deviate. The steep increase of the green curves shows the effects of including heavier states. The agreement between the resulting normalized pressure and the lattice result up to the largest temperatures is good.

In Fig. 6, we show the light quark condensate normalized to its zero-temperature value in different approximations as a function of the temperature. The blue (green) line is the $\mathcal{O}(p^2)$ result without (with) electromagnetic interactions. The yellow (red) line is the $\mathcal{O}(p^4)$ result without (with) electromagnetic interactions. For comparison, we show in black the result from the HRG model. Obviously, χPT is not valid in the entire temperature range shown, but for low temperatures, up to $T \simeq 150$ MeV, it seems to be converging very well and electromagnetic effects are not very large. However, from Figs. 5 and 8 below, it is also clear that χPT alone cannot explain the lattice results beyond approximately 120 MeV.

In Fig. 7, we show the strange quark condensate normalized to its zero-temperature value in different approximations as a function of the temperature. The features are essentially the same as in Fig. 6, except that the electromagnetic effects are somewhat larger in this case.

In Fig. 8, we plot the dimensionless quantity $\Delta_{l,s}$, which is defined as [18]

$$\Delta_{l,s} = \frac{\langle\bar{q}q\rangle_T - \frac{m}{m_s}\langle\bar{s}s\rangle_T}{\langle\bar{q}q\rangle_0 - \frac{m}{m_s}\langle\bar{s}s\rangle_0}. \tag{115}$$

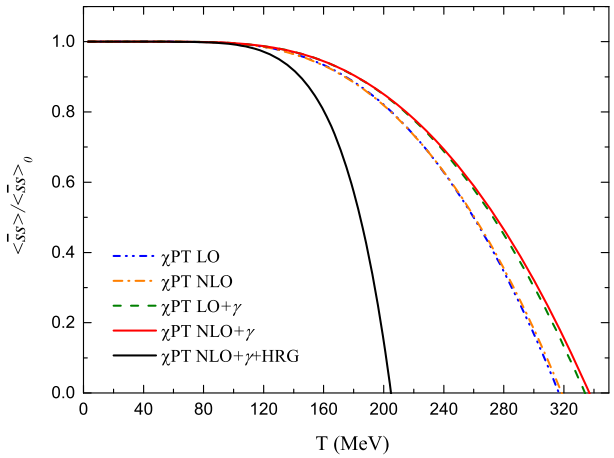

FIG. 7. Normalized strange quark condensate $\langle\bar{s}s\rangle/\langle\bar{s}s\rangle_0$ as a function of the temperature in MeV. See main text for details.

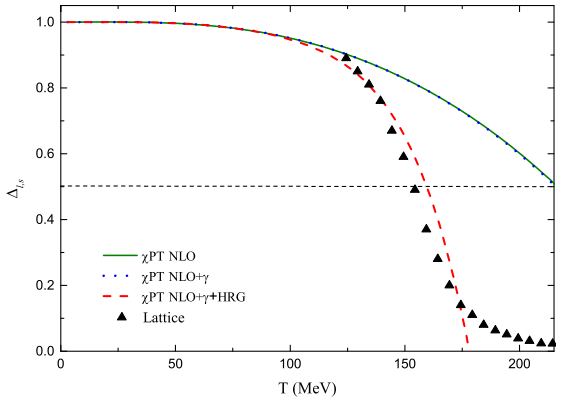

FIG. 8. $\Delta_{l,s}$ as a function of the temperature in MeV. The dotted horizontal curve indicates the value $\Delta_{l,s} = \frac{1}{2}$. See main text for details.

The ratio of light quark mass m and strange quark mass m_s equals $1/30.21$, which is obtained by using the bare values of $m_{\pi,0}$ and $m_{K,0}$. The green (blue) line is the $\mathcal{O}(p^4)$ results without (with) electromagnetic contributions. The red dotted line is for the results combined with the HRG model, which includes all the resonances states below 2.5 GeV in [32]. For comparison, we also plot the lattice results in triangles from Ref. [18]. At low temperatures, the χPT predictions do converge well and the electromagnetic contributions are small. The agreement between the lattice results and the HRG is excellent all the way up to $T \approx 170$ MeV. For QCD with physical quark masses, there is no critical temperature. However, one can define a crossover temperature in different ways. For example, the temperature at which the chiral condensate has decreased to half its vacuum value, or similarly the temperature at which $\Delta_{l,s}$ has decreased to half its vacuum value. It can also be defined as the temperature at which the quark susceptibilities has its peak. Depending on the quantity, the crossover temperature in Ref. [18] is in the 150–170 MeV range. Using the definition $\Delta_{l,s} = \frac{1}{2}$ they obtain $T_{\rm pc} = 157.3$ MeV. Using the same definition, we obtain 160.1 MeV, the dotted line in Fig. 8 indicates this value. This crossover temperature is also very close to $T_{\rm pc} = 161.2$ MeV obtained by a very recent HRG model analysis [23]. Of course, one should bear in mind that the HRG model does not know about the deconfined phase of QCD so the excellent agreement for $T_{\rm pc}$ obtained here, can to some extent be accidental. Likewise, the agreement with lattice data for temperatures above approximately 150 MeV should be taken with a grain of salt for the same reason.

ACKNOWLEDGMENTS

Q. Y. and H. Z. have been supported by the China Scholarship Council. They thank the Department of Physics at NTNU for kind hospitality during their stay.

APPENDIX A: SUM-INTEGRALS

In the imaginary-time formalism, the four-momentum is $P = (p_0, \mathbf{p})$ with $P^2 = p_0^2 + \mathbf{p}^2$ and $p_0 = 2\pi n T$ being the Matsubara frequencies for bosons. Loop integrals involve sums over Matsubara frequencies and integrals over spatial momenta. We use momentum-space dimensional regularization to regulate both infrared and ultraviolet divergences. The sum-integrals are defined as

$$\sum\!\!\!\!\!\!\int_P = T \sum_{p_0 = 2n\pi T} \int_p, \tag{A1}$$

where the sum is over Matsubara frequencies and integrals over momenta are denoted by

$$\int_p = \left(\frac{e^{\gamma_E}\Lambda^2}{4\pi}\right)^{\epsilon} \int \frac{d^d p}{(2\pi)^d}, \tag{A2}$$

where $d = 3 - 2\epsilon$ and Λ is an arbitrary momentum scale that coincides with the renormalization scale in the $\overline{\rm MS}$ scheme. The one-loop integrals that appear in the calculations are of the form

$$I_0'(m^2) = -\sum\!\!\!\!\!\!\int_P \log\,[P^2 + m^2], \tag{A3}$$

$$I_n(m^2) = \sum\!\!\!\!\!\!\int_P \frac{1}{(P^2 + m^2)^n}, \tag{A4}$$

where the prime denotes differentiation with respect to the index n evaluated at $n = 0$. They satisfy the relations

$$\frac{\partial}{\partial m^2} I_0' = -I_1, \qquad \frac{\partial}{\partial m^2} I_n = -n I_{n+1}. \tag{A5}$$

The sum-integral I_n can be evaluated by standard contour-integration techniques. We specifically need

$$I_0'(m^2) = \frac{1}{2(4\pi)^2}\left(\frac{\Lambda}{m}\right)^{2\epsilon}\left[\left(\frac{1}{\epsilon} + \frac{3}{2} + \mathcal{O}(\epsilon)\right) m^4 + 2J_0(\beta m) T^4\right], \tag{A6}$$

$$I_1(m^2) = -\frac{1}{(4\pi)^2}\left(\frac{\Lambda}{m}\right)^{2\epsilon}\left[\left(\frac{1}{\epsilon} + 1 + \frac{\pi^2 + 12}{12}\epsilon\right) m^2 - J_1(\beta m) T^2\right], \tag{A7}$$

where the thermal integrals $J_n(\beta m)$ are defined as

$$J_n(\beta m) = \frac{4e^{\gamma_E\epsilon}\Gamma(\frac{1}{2})}{\Gamma(\frac{5}{2}-n-\epsilon)}\frac{m^{2\epsilon}}{T^{4-2n}}\int_0^\infty n(E_p)\frac{p^{4-2n-2\epsilon}}{E_p}dp, \tag{A8}$$

$n(E_p) = 1/(e^{\beta E_p}-1)$ is the Bose-Einstein (BE) distribution function, β is the inverse of temperature, and $E_p = \sqrt{p^2+m^2}$. The thermal integrals $J_n(x)$ satisfy the recursion relation

$$xJ_n'(x) = 2\epsilon J_n(x) - 2x^2 J_{n+1}(x). \tag{A9}$$

For $\epsilon = 0$ and in the limit $m \to 0$, the thermal integrals behave as

$$J_0 \to \frac{16\pi^4}{45}, \tag{A10}$$

$$J_1 \to \frac{4\pi^2}{3} - 4\pi\beta m - 2\left(\log\frac{\beta m}{4\pi} - \frac{1}{2} + \gamma_E\right)(\beta m)^2, \tag{A11}$$

$$J_2 \to \frac{2\pi}{\beta m} + 2\left(\log\frac{\beta m}{4\pi} + \gamma_E\right). \tag{A12}$$

We notice that $\frac{1}{2}J_0'(0)$ reduces to $\frac{\pi^2}{90}T^4$, which is the Stefan-Boltzmann limit for the pressure of a massless bosonic degree of freedom.

APPENDIX B: EVALUATION OF $I_{\rm sun}(m^2)$

In this appendix, we calculate

$$I_{\rm sun}(m^2) \equiv \sum\!\!\!\!\!\!\int_{PQ} \frac{1}{(P^2+m^2)(Q^2+m^2)(P+Q)^2}. \tag{B1}$$

We use the method of Bugrij and Shadura [38]. The sum-integrals over Euclidean momenta are replaced by integrals over four momenta $p = (p_0, \mathbf{p})$ in Minkowski space, $\sum\!\!\!\!\!\!\int_P \to -i\int_M$, where integrals in Minkowski space are defined as

$$\int_M = \int_{-\infty}^{\infty}\frac{dp_0}{2\pi}\int_p. \tag{B2}$$

The Euclidean propagator is replaced by the Minkowski propagator in the real-time formalism,

$$\frac{1}{P^2+m^2} \to i\left(\frac{i}{p_0^2 - E_p^2 + i\epsilon} + n(|p_0|)2\pi\delta(p_0^2 - E_p^2)\right). \tag{B3}$$

The sum-integral $I_{\rm sun}(m^2)$ is then given by the real part of the resulting expression. Some of the integrals involve one or more factors of the BE distribution. The remaining integrals may conveniently be Wick-rotated back to Euclidean space, $\int_M \to i\int_P$, where the integral is defined as

$$\int_P = \left(\frac{e^{\gamma_E}\Lambda^2}{4\pi}\right)^\epsilon \int \frac{d^{d+1}p}{(2\pi)^{d+1}}, \tag{B4}$$

with $d = 3 - 2\epsilon$. The term with zero thermal factors reads

$$\begin{aligned} I_{\rm sun}^{(0)}(m^2) &= \int_{PQ}\frac{1}{P^2(Q^2+m^2)[(P+Q)^2+m^2]} \\ &= \int_P \frac{1}{P^2}\Pi(P), \end{aligned} \tag{B5}$$

where the superscript (i) $(i = 0, 1, 2, 3)$ of $I_{\rm sun}^{(i)}(m^2)$ denotes the number of BE factors and where we have defined

$$\Pi(P) = \int_Q \frac{1}{(Q^2+m^2)[(P+Q)^2+m^2]}. \tag{B6}$$

The bubble integrals can be calculated e.g. by using Feynman parameters,

$$\Pi(P) = \frac{\pi\csc\epsilon\pi}{\Gamma(1-\epsilon)}\frac{(e^{\gamma_E}\Lambda^2)^\epsilon}{(4\pi)^2}\int_0^1 dx[m^2 + P^2x(1-x)]^{-\epsilon}. \tag{B7}$$

Integrating first over four-momenta P and then over x yields

$$I_{\rm sun}^{(0)}(m^2) = \frac{\pi\csc\epsilon\pi}{\Gamma(1-\epsilon)}\frac{(e^{\gamma_E}\Lambda^2)^\epsilon}{(4\pi)^2}\int_0^1 dx\int_P\frac{1}{P^2}[m^2+P^2x(1-x)]^{-\epsilon} = -\frac{m^2}{(4\pi)^4}\left(\frac{\Lambda}{m}\right)^{4\epsilon}e^{2\gamma_E\epsilon}\frac{(d-1)\pi^2\csc^2\epsilon\pi}{2(d-2)\Gamma^2(2-\epsilon)}. \tag{B8}$$

Expanding in powers of ϵ through order ϵ^0 gives

$$I_{\rm sun}^{(0)}(m^2) = -\frac{m^2}{(4\pi)^4}\left(\frac{\Lambda}{m}\right)^{4\epsilon}\left[\frac{1}{\epsilon^2} + \frac{3}{\epsilon} + 7 + \frac{\pi^2}{6} + \mathcal{O}(\epsilon)\right]. \tag{B9}$$

The terms with one thermal factor are

$$I^{(1)}_{\rm sun}(m^2) = \int_M n(|p_0|)2\pi\delta(p_0^2-p^2)\int_Q \frac{1}{(Q^2+m^2)[(P+Q)^2+m^2]}\bigg|_{P^2=0} + 2\int_M n(|p_0|)2\pi\delta(p_0^2-E_p^2) \times \int_Q \frac{1}{(Q^2+m^2)(P+Q)^2}\bigg|_{P^2=-m^2}. \tag{B10}$$

The integral over Q in the first term is $\Pi(P)$ in Eq. (B7), evaluated at $P^2=0$. The integral over Q in the second term can be evaluated in the same way. Expanding the resulting expressions in powers of ϵ yields

$$\int_Q \frac{1}{(Q^2+m^2)[(P+Q)^2+m^2]} = \frac{1}{(4\pi)^2}\left(\frac{\Lambda}{m}\right)^{2\epsilon}\left[\frac{1}{\epsilon}-\int_0^1 \log\frac{m^2+x(1-x)P^2}{m^2}dx+\mathcal{O}(\epsilon)\right] = \frac{1}{(4\pi)^2}\left(\frac{\Lambda}{m}\right)^{2\epsilon}\left[\frac{1}{\epsilon}+\mathcal{O}(\epsilon)\right], \tag{B11}$$

$$\int_Q \frac{1}{(Q^2+m^2)(P+Q)^2} = \frac{1}{(4\pi)^2}\left(\frac{\Lambda}{m}\right)^{2\epsilon}\left[\frac{1}{\epsilon}-\int_0^1 \log\frac{xm^2+x(1-x)P^2}{m^2}dx+\mathcal{O}(\epsilon)\right] = \frac{1}{(4\pi)^2}\left(\frac{\Lambda}{m}\right)^{2\epsilon}\left[\frac{1}{\epsilon}+2+\mathcal{O}(\epsilon)\right]. \tag{B12}$$

Substituting Eqs. (B11) and (B12) into Eq. (B10) and integrating over p_0 yields

$$I^{(1)}_{\rm sun}(m^2) = \frac{1}{(4\pi)^2}\left(\frac{\Lambda}{m}\right)^{2\epsilon}\int_p\left[\frac{n(p)}{p}\frac{1}{\epsilon}+\frac{2n(E_p)}{E_p}\left(\frac{1}{\epsilon}+2\right)\right]. \tag{B13}$$

The terms with two thermal factors are

$$I^{(2)}_{\rm sun}(m^2) = \int_M n(|p_0|)2\pi\delta(p_0^2-E_p^2)\int_M n(|q_0|)2\pi\delta(q_0^2-E_q^2)\frac{1}{(p_0+q_0)^2-(\mathbf{p}+\mathbf{q})^2} + 2\int_M n(|p_0|)2\pi\delta(p_0^2-p^2)\int_M n(|q_0|)2\pi\delta(q_0^2-E_q^2)\frac{1}{(p_0+q_0)^2-(\mathbf{p}+\mathbf{q})^2-m^2}. \tag{B14}$$

This integral is convergent in three dimensions so we set $\epsilon=0$. We first integrate over p_0 and q_0, which yields

$$I^{(2)}_{\rm sun}(m^2) = \frac{1}{2}\int_{pq}\frac{n(E_p)n(E_q)}{E_pE_q}\left[\frac{1}{(E_p+E_q)^2-(\mathbf{p}+\mathbf{q})^2}+\frac{1}{(E_p-E_q)^2-(\mathbf{p}+\mathbf{q})^2}\right] + \int_{pq}\frac{n(p)n(E_q)}{pE_q}\left[\frac{1}{(p+E_q)^2-(\mathbf{p}+\mathbf{q})^2-m^2}+\frac{1}{(p-E_q)^2-(\mathbf{p}+\mathbf{q})^2-m^2}\right]. \tag{B15}$$

Averaging over the angle between $\mathbf{p}$ and $\mathbf{q}$ gives

$$I^{(2)}_{\rm sun}(m^2) = \frac{8}{(4\pi)^4}\int_0^\infty \frac{pn(E_p)qn(E_q)}{E_pE_q}\log\frac{(p-q)^2}{(p+q)^2}\,dpdq, \tag{B16}$$

where we notice that the angular average of the term in the second line of Eq. (B15) vanishes. Finally, the term with three thermal factors, $I^{(3)}_{\rm sun}(m^2)$, is purely imaginary and is dropped. Adding Eqs. (B9), (B13), and (B16), we obtain the result for the setting-sun diagram

$$I_{\rm sun}(m^2) = -\frac{m^2}{(4\pi)^4}\left(\frac{\Lambda}{m}\right)^{4\epsilon}\left[\frac{1}{\epsilon^2}+\frac{3}{\epsilon}+7+\frac{\pi^2}{6}\right]+\frac{1}{(4\pi)^2}\left(\frac{\Lambda}{m}\right)^{2\epsilon}\int_p\left[\frac{n(p)}{p}\frac{1}{\epsilon}+\frac{2n(E_p)}{E_p}\left(\frac{1}{\epsilon}+2\right)\right] + \frac{8}{(4\pi)^4}\int_0^\infty\frac{pn(E_p)qn(E_q)}{E_pE_q}\log\frac{(p-q)^2}{(p+q)^2}\,dpdq. \tag{B17}$$

APPENDIX C: ONE-LOOP VACUUM ENERGY

In this appendix, we calculate the vacuum energy V including electromagnetic effects. From V it is easy to derive the one-loop corrections to the quark condensates that are needed in our finite-temperature formulas. The $\mathcal{O}(p^2)$ contribution is

$$V_0 = -\frac{1}{2}f^2(m_{\pi,0}^2 + 2m_{K,0}^2). \tag{C1}$$

The $\mathcal{O}(p^4)$ contribution from the loops is

$$\begin{aligned} V_1 = {} & \frac{1}{2}\int_P \log[P^2 + m_{\pi,0}^2] + \int_P \log[P^2 + m_{\pi^\pm,0}^2] \\ & + \int_P \log[P^2 + m_{K^\pm,0}^2] + \int_P \log[P^2 + m_{K,0}^2] \\ & + \frac{1}{2}\int_P \log[P^2 + m_{\eta,0}^2] + (d-1)\int_P \log[P^2], \end{aligned} \tag{C2}$$

where the last term comes from the photons and ghost and vanishes at zero temperature. The $\mathcal{O}(p^4)$ counterterm contribution is

$$\begin{aligned} V_1^{\mathrm{ct}} = {} & -(4L_6 - 2L_8 - H_2)(m_{\pi,0}^2 + 2m_{K,0}^2)^2 - 4(2L_8 + H_2)(m_{\pi,0}^4 + 2m_{K,0}^4) - \frac{4e^2f^2m_{\pi,0}^2}{3}\left[K_7 + K_8 + \frac{4}{3}K_9 + \frac{4}{3}K_{10}\right] \\ & - \frac{8e^2f^2m_{K,0}^2}{3}\left[K_7 + K_8 + \frac{1}{3}K_9 + \frac{1}{3}K_{10}\right] - \frac{4e^4f^4}{9}[K_{15} + K_{16} + K_{17}]. \end{aligned} \tag{C3}$$

After renormalization, we find the vacuum energy for three-flavor χPT to $\mathcal{O}(p^4)$ including electromagnetic effects.

$$\begin{aligned} V_{0+1} = {} & -\frac{1}{2}f^2(m_{\pi,0}^2 + 2m_{K,0}^2) - (4L_6^r - 2L_8^r - H_2^r)(m_{\pi,0}^2 + 2m_{K,0}^2)^2 - 4(2L_8^r + H_2^r)(m_{\pi,0}^4 + 2m_{K,0}^4) \\ & - \frac{m_{\pi,0}^4}{4(4\pi)^2}\left(\log\frac{\Lambda^2}{m_{\pi,0}^2} + \frac{1}{2}\right) - \frac{m_{\pi^\pm,0}^4}{2(4\pi)^2}\left(\log\frac{\Lambda^2}{m_{\pi^\pm,0}^2} + \frac{1}{2}\right) - \frac{m_{K^\pm,0}^4}{2(4\pi)^2}\left(\log\frac{\Lambda^2}{m_{K^\pm,0}^2} + \frac{1}{2}\right) \\ & - \frac{m_{K,0}^4}{2(4\pi)^2}\left(\log\frac{\Lambda^2}{m_{K,0}^2} + \frac{1}{2}\right) - \frac{m_{\eta,0}^4}{4(4\pi)^2}\left(\log\frac{\Lambda^2}{m_{\eta,0}^2} + \frac{1}{2}\right) - \frac{4e^2f^2m_{\pi,0}^2}{3}\left[K_7^r + K_8^r + \frac{4}{3}K_9^r + \frac{4}{3}K_{10}^r\right] \\ & - \frac{8e^2f^2m_{K,0}^2}{3}\left[K_7^r + K_8^r + \frac{1}{3}K_9^r + \frac{1}{3}K_{10}^r\right] - \frac{4e^4f^4}{9}[K_{15}^r + K_{16}^r + K_{17}^r]. \end{aligned} \tag{C4}$$

The light and s-quark condensates to $\mathcal{O}(p^4)$ in the vacuum are

$$\begin{aligned} \langle\bar{q}q\rangle_0 = {} & -2f^2B_0\left[1 + \frac{m_{\pi,0}^2}{f^2}\left(16L_6^r + 8L_8^r + 4H_2^r + \frac{1}{2(4\pi)^2}\log\frac{\Lambda^2}{m_{\pi,0}^2}\right) + \frac{m_{K,0}^2}{f^2}\left(32L_6^r + \frac{1}{2(4\pi)^2}\log\frac{\Lambda^2}{m_{K,0}^2}\right)\right. \\ & \left. + \frac{m_{\pi^\pm,0}^2}{(4\pi)^2f^2}\log\frac{\Lambda^2}{m_{\pi^\pm,0}^2} + \frac{m_{K^\pm,0}^2}{2(4\pi)^2f^2}\log\frac{\Lambda^2}{m_{K^\pm,0}^2} + \frac{m_{\eta,0}^2}{6(4\pi)^2f^2}\log\frac{\Lambda^2}{m_{\eta,0}^2}\right] \\ & - \frac{16e^2f^2B_0}{3}\left(K_7^r + K_8^r + \frac{5}{6}K_9^r + \frac{5}{6}K_{10}^r\right), \end{aligned} \tag{C5}$$

$$\begin{aligned} \langle\bar{s}s\rangle_0 = {} & -f^2B_0\left[1 + \frac{4m_{\pi,0}^2}{f^2}(4L_6^r - 2L_8^r - H_2^r) + \frac{m_{K,0}^2}{f^2}\left(32L_6^r + 16L_8^r + 8H_2^r + \frac{1}{(4\pi)^2}\log\frac{\Lambda^2}{m_{K,0}^2}\right)\right. \\ & \left. + \frac{m_{K^\pm,0}^2}{(4\pi)^2f^2}\log\frac{\Lambda^2}{m_{K^\pm,0}^2} + \frac{2m_{\eta,0}^2}{3(4\pi)^2f^2}\log\frac{\Lambda^2}{m_{\eta,0}^2}\right] - \frac{8e^2f^2B_0}{3}\left(K_7^r + K_8^r + \frac{1}{3}K_9^r + \frac{1}{3}K_{10}^r\right). \end{aligned} \tag{C6}$$

Note that quark condensates depend on the coupling H_2^r, which is unphysical in the sense that it arises from a contact term in the $\mathcal{O}(p^4)$ Lagrangian.

APPENDIX D: MESON MASSES AND PION-DECAY CONSTANT

In this appendix, we list the meson masses to one-loop order including the leading electromagnetic effects, i.e. through e^2. The meson masses without electromagnetic corrections were calculated in Ref. [3], while electromagnetism was included in Ref. [9]. The meson masses without electromagnetic corrections are

$$M_\pi^2 = m_{\pi,0}^2\left[1-\frac{m_{\pi,0}^2}{f^2}\left(8L_4^r+8L_5^r-16L_6^r-16L_8^r+\frac{1}{2(4\pi)^2}\log\frac{\Lambda^2}{m_{\pi,0}^2}\right)-\frac{m_{K,0}^2}{f^2}(16L_4^r-32L_6^r)+\frac{m_{\eta,0}^2}{6(4\pi)^2f^2}\log\frac{\Lambda^2}{m_{\eta,0}^2}\right], \tag{D1}$$

$$M_K^2 = m_{K,0}^2\left[1-\frac{m_{\pi,0}^2}{f^2}(8L_4^r-16L_6^r)-\frac{m_{K,0}^2}{f^2}(16L_4^r+8L_5^r-32L_6^r-16L_8^r)-\frac{m_{\eta,0}^2}{3(4\pi)^2f^2}\log\frac{\Lambda^2}{m_{\eta,0}^2}\right], \tag{D2}$$

$$\begin{aligned}M_\eta^2 = m_{\eta,0}^2\Bigg[&1-\frac{m_{\pi,0}^2}{f^2}\left(8L_4^r-16L_6^r+\frac{1}{6(4\pi)^2}\log\frac{\Lambda^2}{m_{\eta,0}^2}\right)-\frac{m_{K,0}^2}{f^2}\left(16L_4^r-32L_6^r+\frac{1}{(4\pi)^2}\log\frac{\Lambda^2}{m_{K,0}^2}\right)\\&-\frac{m_{\eta,0}^2}{f^2}\left(8L_5^r-\frac{2}{3(4\pi)^2}\log\frac{\Lambda^2}{m_{\eta,0}^2}\right)\Bigg]+L_7^r\frac{128(m_{\pi,0}^2-m_{K,0}^2)^2}{3f^2}+L_8^r\frac{16}{3f^2}(3m_{\pi,0}^4-8m_{\pi,0}^2m_{K,0}^2+8m_{K,0}^4)\\&+\frac{m_{\pi,0}^4}{2(4\pi)^2f^2}\log\frac{\Lambda^2}{m_{\pi,0}^2}-\frac{m_{\pi,0}^2m_{K,0}^2}{3(4\pi)^2f^2}\log\frac{\Lambda^2}{m_{K,0}^2}.\end{aligned} \tag{D3}$$

After including the one-loop χPT contribution to meson masses and electromagnetic effects up to order e^2, the charged and neutral meson masses are

$$\begin{aligned}m_{\pi^0}^2 = M_\pi^2 &+ e^2m_{\pi,0}^2\left(-\frac{8}{3}K_1^r-\frac{8}{3}K_2^r+4K_3^r-2K_4^r-\frac{20}{9}K_5^r-\frac{20}{9}K_6^r+\frac{8}{3}K_7^r+\frac{8}{3}K_8^r+\frac{20}{9}K_9^r+\frac{20}{9}K_{10}^r\right)\\&+2\frac{Ce^2m_{\pi,0}^2}{(4\pi)^2f^4}\left(1-\log\frac{\Lambda^2}{m_{\pi,0}^2}\right),\end{aligned} \tag{D4}$$

$$\begin{aligned}m_{\pi^\pm}^2 = M_\pi^2 &+ e^2m_{\pi,0}^2\left(-\frac{8}{3}K_1^r-\frac{8}{3}K_2^r-\frac{20}{9}K_5^r-\frac{20}{9}K_6^r+\frac{8}{3}K_7^r+\frac{20}{3}K_8^r+\frac{20}{9}K_9^r+\frac{92}{9}K_{10}^r+8K_{11}^r\right)\\&+8e^2m_{K,0}^2K_8^r+\frac{e^2m_{\pi,0}^2}{(4\pi)^2}\left(4+3\log\frac{\Lambda^2}{m_{\pi,0}^2}\right)-L_4^r\frac{16Ce^2}{f^4}(m_{\pi,0}^2+2m_{K,0}^2)-L_5^r\frac{16Ce^2m_{\pi,0}^2}{f^4}\\&+4\frac{Ce^2m_{\pi,0}^2}{(4\pi)^2f^4}\log\frac{\Lambda^2}{m_{\pi,0}^2}+2\frac{Ce^2m_{K,0}^2}{(4\pi)^2f^4}\log\frac{\Lambda^2}{m_{K,0}^2},\end{aligned} \tag{D5}$$

$$\begin{aligned}m_{K^\pm}^2 = M_K^2 &+ e^2m_{K,0}^2\left(-\frac{8}{3}K_1^r-\frac{8}{3}K_2^r-\frac{20}{9}K_5^r-\frac{20}{9}K_6^r+\frac{8}{3}K_7^r+\frac{32}{3}K_8^r+\frac{8}{9}K_9^r+\frac{80}{9}K_{10}^r+8K_{11}^r\right)\\&+e^2m_{\pi,0}^2\left(4K_8^r+\frac{4}{3}K_9^r+\frac{4}{3}K_{10}^r\right)+\frac{e^2m_{K,0}^2}{(4\pi)^2}\left(4+3\log\frac{\Lambda^2}{m_{K,0}^2}\right)-L_4^r\frac{16Ce^2}{f^4}(m_{\pi,0}^2+2m_{K,0}^2)\\&-L_5^r\frac{16Ce^2m_{K,0}^2}{f^4}+2\frac{Ce^2m_{\pi,0}^2}{(4\pi)^2f^4}\log\frac{\Lambda^2}{m_{\pi,0}^2}+4\frac{Ce^2m_{K,0}^2}{(4\pi)^2f^4}\log\frac{\Lambda^2}{m_{K,0}^2},\end{aligned} \tag{D6}$$

$$m_{K^0}^2 = M_K^2+\frac{8}{9}e^2m_{K,0}^2(-3K_1^r-3K_2^r-K_5^r-K_6^r+3K_7^r+3K_8^r+K_9^r+K_{10}^r), \tag{D7}$$

$$\begin{aligned}m_\eta^2 = M_\eta^2 &+ e^2m_{\eta,0}^2\left(-\frac{8}{3}K_1^r-\frac{8}{3}K_2^r+\frac{4}{3}K_3^r-\frac{2}{3}K_4^r-\frac{4}{3}K_5^r-\frac{4}{3}K_6^r+\frac{8}{3}K_7^r+\frac{8}{3}K_8^r+\frac{8}{9}K_9^r+\frac{8}{9}K_{10}^r\right)\\&+\frac{4}{9}e^2m_{\pi,0}^2(K_9^r+K_{10}^r)-\frac{2}{3}\frac{Ce^2m_{\pi,0}^2}{(4\pi)^2f^4}\left(1-\log\frac{\Lambda^2}{m_{\pi,0}^2}\right)+\frac{Ce^2m_{K,0}^2}{3(4\pi)^2f^4}\left(1-4\log\frac{\Lambda^2}{m_{K,0}^2}\right).\end{aligned} \tag{D8}$$

Finally, including electromagnetic effects, the neutral pion-decay constant f_{π^0} is

$$f_{\pi^0} = f\left[1 + (4L_4^r + 4L_5^r)\frac{m_{\pi,0}^2}{f^2} + 8L_4^r\frac{m_{K,0}^2}{f^2} + e^2\left(\frac{4}{3}K_1^r + \frac{4}{3}K_2^r - 2K_3^r + K_4^r + \frac{10}{9}K_5^r + \frac{10}{9}K_6^r\right) + \frac{m_{\pi^\pm,0}^2}{(4\pi)^2 f^2}\log\frac{\Lambda^2}{m_{\pi^\pm,0}^2} + \frac{m_{K^\pm,0}^2}{4(4\pi)^2 f^2}\log\frac{\Lambda^2}{m_{K^\pm,0}^2} + \frac{m_{K,0}^2}{4(4\pi)^2 f^2}\log\frac{\Lambda^2}{m_{K,0}^2}\right]. \tag{D9}$$

[1] S. Weinberg, Physica (Amsterdam) **96A**, 327 (1979).
[2] J. Gasser and H. Leutwyler, Ann. Phys. (N.Y.) **158**, (142) (1984).
[3] J. Gasser and H. Leutwyler, Nucl. Phys. **B250**, 465 (1985).
[4] H. W. Fearing and S. Scherer, Phys. Rev. D **53**, 315 (1996).
[5] J. Bijnens, G. Colangelo, and G. Ecker, Ann. Phys. (N.Y.) **280**, 100 (2000).
[6] J. Bijnens, G. Colangelo, and G. Ecker, J. High Energy Phys. 02 (1999) 020.
[7] J. Bijnens and G. Ecker, Annu. Rev. Nucl. Part. Sci. **64**, 149 (2014).
[8] G. Ecker, J. Gasser, A. Pich, and E. de Rafael, Nucl. Phys. **B321**, 311 (1989).
[9] R. Urech, Nucl. Phys. **B433**, 234 (1995).
[10] U.-G. Meissner, G. Müller, and S. Steininger, Phys. Lett. B **406** (1997).
[11] U.-G. Meissner, G. Müller, and S. Steininger, Phys. Lett. B **407**, 454(E) (1997).
[12] M. Knecht and R. Urech, Nucl. Phys. **B519**, 329 (1998).
[13] J. Gasser and H. Leutwyler, Phys. Lett. B **184**, 83 (1987).
[14] J. Gasser and H. Leutwyler, Phys. Lett. B **188**, 477 (1987).
[15] P. Gerber and H. Leutwyler, Nucl. Phys. **B321**, 387 (1989).
[16] Y. Aoki, Z. Fodor, S. Katz, and K. Szabo, Phys. Lett. B **643**, 46 (2006).
[17] Y. Aoki, S. Borsanyi, S. Dürr, Z. Fodor, S. D. Katz, S. Krieg and K. K. Szabo, J. High Energy Phys. 06 (2009) 088.
[18] S. Borsanyi *et al.* (Wuppertal-Budapest Collaboration), J. High Energy Phys. 09 (2010) 073.
[19] A. Bazavov, T. Bhattacharya, M. Cheng, C. DeTar, H. Ding *et al.*, Phys. Rev. D **85**, 054503 (2012).
[20] F. Karsch, K. Redlich, and A. Tawfik, Eur. Phys. J. C **29**, 549 (2003).
[21] F. Karsch, K. Redlich, and A. Tawfik, Phys. Lett. B **571**, 67 (2003).
[22] J. Jankowski, D. Blaschke, and M. Spaliński, Phys. Rev. D **87**, 105018 (2013).
[23] D. Biswas, P. Petreczky, and S. Sharma, Phys. Rev. C **106**, 045203 (2022).
[24] A. Nicola and R. Torres Andrés, Phys. Rev. D **83**, 076005 (2011).
[25] A. Nicola and R. Torres Andrés, Phys. Rev. D **89**, 116009 (2014).
[26] E. Braaten and R. D. Pisarski, Phys. Rev. D **42**, 2156 (1990).
[27] E. Braaten and R. D. Pisarski, Nucl. Phys. **B337**, 569 (1990).
[28] E. Braaten and R. D. Pisarski, Phys. Rev. D **45**, R1827 (1992).
[29] J. Frenkel and J. C. Taylor, Nucl. Phys. **B374**, 156 (1992).
[30] E. Braaten, Can. J. Phys. **71**, 215 (1993).
[31] J. Gasser, A. Rusetsky, and I. Scimemi, Eur. J. Phys. C **32**, 97 (2003).
[32] P. A. Zyla *et al.* (Particle Data Group), Prog. Theor. Exp. Phys. **2020**, 083C01 (2020).
[33] J. Martin Camalich, L. S. Geng, and M. J. Vicente Vacas, Phys. Rev. D **82**, 074504 (2010).
[34] M. Jamin, Phys. Lett. B **538**, 71 (2002).
[35] M. Gorghetto and G. Villadoro, J. High Energy Phys. 03 (2019) 033.
[36] J. Bijnens and J. Prades, Nucl. Phys. **B490**, 239 (1997).
[37] G. Endrodi, J. High Energy Phys. 04 (2013) 023.
[38] A. I. Bugrij and V. N. Shadura, arXiv:hep-th/9510232.